

Potential of land-based climate change mitigation strategies on abandoned cropland

Maren H. Gvein¹[✉], Xiangping Hu¹, Jan S. Næss¹, Marcos D. B. Watanabe¹, Otávio Cavalett¹, Maxime Malbranque¹, Georg Kindermann² & Francesco Cherubini¹[✉]

Natural revegetation, afforestation, and lignocellulosic crops for bioenergy, possibly coupled with a developing technology like carbon capture and storage, are the most common land-based climate change mitigation options. However, they can compete for land and threaten food security or nature conservation. Using abandoned cropland for their deployment can minimize these risks, but associated potentials are unclear. Here, we compare alternative land-based mitigation options by integrating historical and future (up to 2050) abandoned cropland with site-specific biomass yields and life-cycle emissions. Considering natural revegetation in biodiversity priority areas and different measures in the remaining land can achieve a mitigation potential of 0.8–4.0 GtCO₂-equivalents yr⁻¹ (2–11% of 2021 global CO₂ emissions). Afforestation generally provides larger climate benefits than bioenergy, but bioenergy with carbon capture and storage delivers the highest mitigation in most locations. Overall, these results offer refined estimates of mitigation potentials from abandoned cropland and highlight opportunities for context-specific mitigation measures.

¹Industrial Ecology Programme, Department of Energy and Process Engineering, Norwegian University of Science and Technology, Trondheim, Norway.

²International Institute for Applied Systems Analysis (IIASA), Laxenburg, Austria. ✉email: maren.h.gvein@ntnu.no; francesco.cherubini@ntnu.no

Land-based Carbon Dioxide Removal (CDR) is a key component of climate change mitigation scenarios^{1,2}. Bioenergy (BE) coupled or not with carbon capture and storage (BECCS), afforestation (AF) and natural vegetation regrowth (NR) are among the options with the largest mitigation potential. Large-scale AF is considered an inexpensive CDR to capture a large fraction of anthropogenic CO₂ emissions^{3,4}. Estimates of its sequestration potential range between 0.5 and 10.1 GtCO₂ yr⁻¹ (with realistic figures around 3 GtCO₂ yr⁻¹)¹, with an associated expansion of global forest areas in 2100 of up to 1000 million hectares (Mha)⁵. NR is the most cost-effective nature-based solution⁶ for nature conservation while capturing atmospheric carbon⁷. In about 30 years of large-scale deployment of natural vegetation regrowth, up to 1.08 GtC yr⁻¹ can be accumulated in aboveground biomass growing on land areas (349 Mha) identified by the country-level commitments to the Bonn Challenge and Paris Agreement⁸. BE is not a CDR option, but it can contribute to climate change mitigation by emission reduction through substitution of fossil fuels. BECCS, a technology that is still at a pre-commercial stage and not deployed at scale, is a CDR option that co-delivers energy and negative emissions^{9–11}. The BECCS mitigation potential in 2100 is estimated at 0.4–11.3 GtCO₂ yr⁻¹, with 0.4–5 GtCO₂ yr⁻¹ identified as a likely sustainable potential¹. Across all Shared Socio-economic Pathways (SSPs)^{12–17}, BE is expected to supply 38–310 EJ yr⁻¹ of primary energy in 2050. BECCS gains importance in future scenarios that are strongly dependent on technical solutions to mitigate climate change. For example, BECCS dominates land-based CDR in SSP5: annual biomass demand from lignocellulosic bioenergy crops in 2100 is about 10 thousand tons in SSP5-4.5, and more than 20 thousand tons in SSP5-2.6⁵.

For all mitigation options, land availability is a key constraint for the delivery of large-scale potentials, as competition with food production represents a major trade-off^{18,19}. Achieving the mitigation potentials indicated above requires dietary shifts towards plant-based diets and efficiency improvements in the agri-food sector to release large areas of grazing lands and croplands from food and feed production, and dedicate them to the implementation of CDR. Utilizing abandoned cropland for CDR is thus a cornerstone for sustainable mitigation in future scenarios^{20–22}. At a local level, cropland abandonment is a result of primarily economic, social, and political drivers^{23,24} and ecological consequences are usually positive²⁵. Abandoned cropland typically reverts to natural grasslands or forests²⁶, thereby sequestering atmospheric CO₂ at minimal costs^{27,28}. Both AF and BE are competitive alternatives to NR because abandoned cropland is usually accessible relative to more remote areas and does not require intensive site preparation. When managed sustainably, perennial grasses grown for bioenergy and afforestation can deliver considerable co-benefits relative to cropland, such as enhanced biodiversity, reduced pollution, increased soil health, higher water holding capacity, and regional cooling^{6,29,30}.

The land-based option that can achieve the largest climate change mitigation potential for one hectare of land in different locations across the globe is still unclear. Most of the existing studies typically have either a coarse resolution or a region-specific scope, only focusing on individual potentials of BE and BECCS^{21,31}, AF^{3,19}, or NR^{6,8}, or compare two options at the time^{10,32,33}. Actual carbon mitigation benefits vary widely and depend on multiple local factors³⁴. The climate change mitigation potential of AF depends on tree species selection and local climate², and the one from BE is highly dependent on crop yields and conversion technology^{10,11,35,36}. Tree planting on abandoned cropland can accumulate more carbon than natural regeneration at high latitudes^{33,37}. Relative to BE, the carbon accumulation in natural succession generally achieves lower carbon savings, but

results are sensitive to bioenergy conversion efficiency^{32,38}. These comparisons are often site-specific^{3,39} or, when global, they lack high-spatial resolution as they rely on average estimates of tree growth rates^{32,38} or are stemming from top-down econometric models that make implicit assumptions about land availability with simplified representations of biophysical constraints^{1,36}. Studies comparing multiple CDR options on a global scale using site-specific data from bottom-up perspectives are missing, and we lack estimates of potentials and optimal distribution of CDR options under a consistent framework. To bridge regional development plans with global goals, the international community requires clarity on the mitigation potentials that can be realistically expected, and how land-based mitigation options perform in different local contexts and relative to each other.

In this study, we perform a bottom-up and spatially explicit quantification of the climate change mitigation potential of CDR measures (NR, AF, and BECCS) and BE on historical and future estimates of abandoned cropland. Potentials are estimated until 2050, as the mitigation efforts achieved in the next decades are crucial for climate change stabilization^{40,41}. Abandoned cropland is identified using time-series from remote-sensing land cover products^{42,43}. The land that falls within the top 15% of priority areas for biodiversity protection is reserved to NR for nature conservation to support the achievement of the Aichi Biodiversity Target 15⁷. In the rest of abandoned cropland, the climate change mitigation potentials of NR, AF, BE, or BECCS are compared. Although BE without CCS is not a CDR method, it is included in our analysis as it is one of the most discussed land-based mitigation options. In the cases of production of perennial grasses for bioenergy, both yields under rainfed conditions and with irrigation (only in areas not affected by water scarcity) are considered. Results are produced by integrating spatially explicit datasets of biomass yields tailored to local conditions and contributions from life-cycle emissions of the production processes, when relevant (i.e., BE, BECCS, and tree planting).

Results and discussion

Abandoned cropland and mitigation potentials. A historical abandoned cropland (AC) of 98 Mha is identified between 1992 and 2018 (Fig. 1a), of which approximately 30 Mha (31%) is located inside priority areas for biodiversity conservation (Supplementary Fig. 1a) and 15 Mha (16%) within areas at risk of water scarcity (see Supplementary Table 1). Compared to the 83 Mha of previously mapped abandoned croplands^{21,44} in 1992–2015, the rate of cropland abandonment has increased, going from 3.6 Mha yr⁻¹ between 1992 and 2015 to 4.8 Mha yr⁻¹ between 2015 and 2018. In general, cropland abandonment mostly occurred in Europe, Central and coastal parts of South America, equatorial Africa, and Southeast Asia.

Future cropland abandonment by 2050 is projected considering a moderate continuous trend in abandonment (named AC4, Fig. 1b) or a relatively larger expansion (named AC8, Fig. 1c). The total abandoned cropland is 139 Mha (+41 Mha relative to AC) in AC4 and 161 Mha (+63 Mha) in AC8. The amount of abandoned cropland located in priority areas is 40 Mha in AC4 (Supplementary Fig. 1b) and 45 Mha in AC8 (Supplementary Fig. 1c). As the future expansion of abandoned cropland relies on the nearest neighbor method (see Methods), the two options show similar spatial patterns as the historical abandoned cropland. The average rate of cropland abandonment between 2018 and 2050 is 1.3 Mha yr⁻¹ for AC4 and 2.0 Mha yr⁻¹ for AC8, which are more conservative than the historical trends. Out of the possible future land use scenarios of SSP-RCP combinations provided by the Global Change Assessment Model (GCAM)⁴⁵, our global estimates of future abandoned cropland

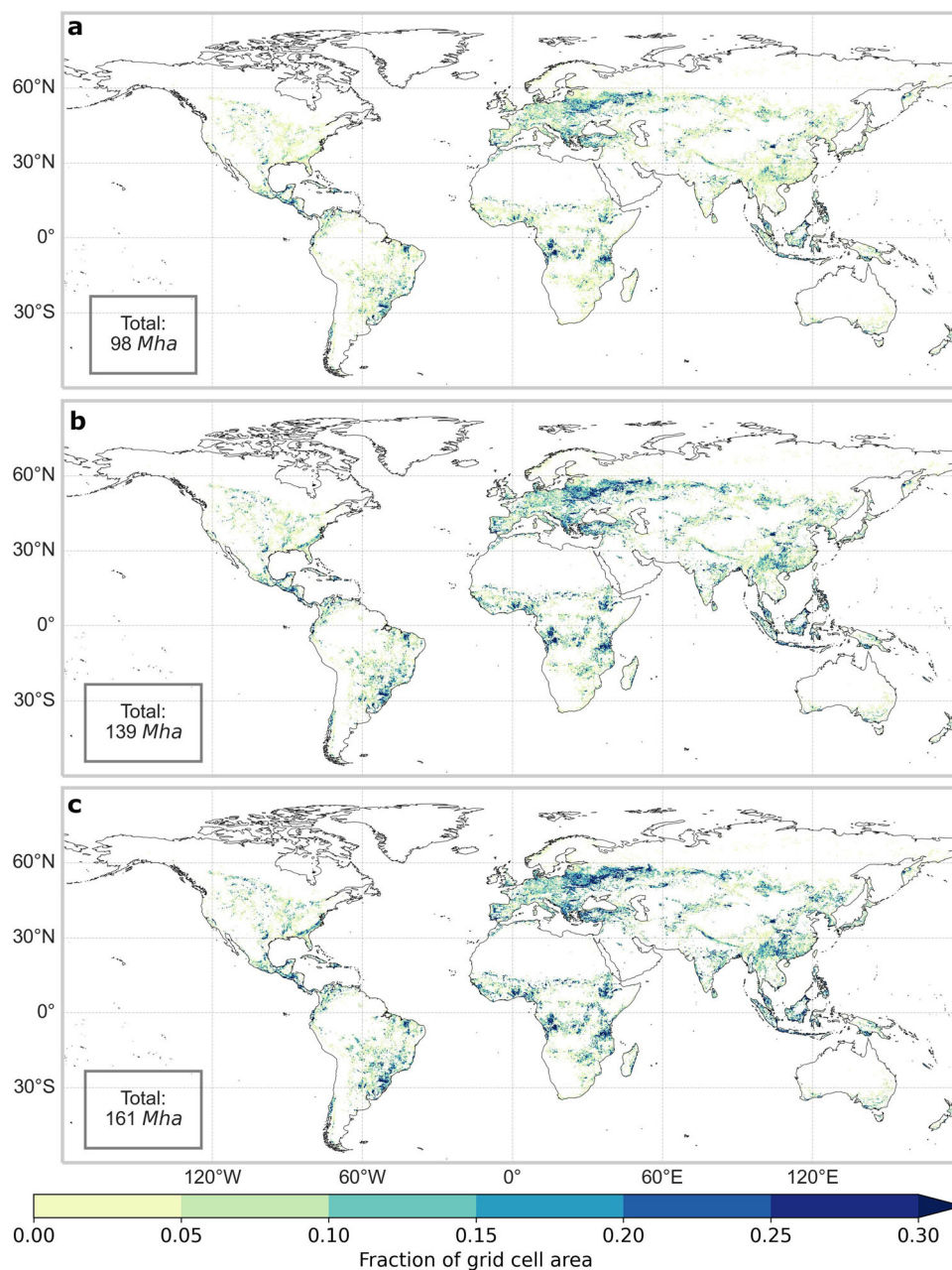


Fig. 1 Global historical and future estimates of abandoned cropland as fraction of a grid cell. Historical cropland abandonment (AC) from 1992 to 2018 (a). Historical plus future estimates of cropland abandonment in the AC4 (b) and AC8 (c) scenarios by 2050. Abandoned cropland in future scenarios only are shown in Supplementary Fig. 2.

are closer to SSP2-RCP4.5 (AC4) and SSP4-RCP6.0 (AC8) projections, that estimate 41 and 84 Mha of cropland abandonment by 2050, respectively (Supplementary Fig. 2).

The annual average energy and climate change mitigation potentials of the different mitigation options are summarized in Table 1. As a benchmark, total anthropogenic emissions in 2021 were 40 GtCO₂ yr⁻¹, net zero emissions in 2050 would require a yearly decrease in emissions of 1.4 GtCO₂ yr⁻¹⁴⁶, and the global primary energy consumption in 2019 was 624 EJ⁴⁷.

Primary bioenergy potentials from rainfed crops range from 19 EJ yr⁻¹ to 33 EJ yr⁻¹ on 67–115 Mha of abandoned cropland outside priority areas, and from 25 EJ yr⁻¹ to 44 EJ yr⁻¹ for crops with mixed water supply (where irrigation can be only applied in areas of low water scarcity). In the latter case, 92% of the potential comes from irrigated crops (on 56–96 Mha). Final bioenergy

potentials estimated as the sum of Fisher-Tropsch (FT) diesel and second generation (2G) ethanol are 9–16 EJ yr⁻¹ for rainfed crops, and 12–21 EJ yr⁻¹ for crops with mixed water supply. Net mitigation potentials with rainfed water supply are 0.6–1.1 GtCO₂ yr⁻¹ for BE and 1.7–2.9 GtCO₂ yr⁻¹ for BECCS. The mixed water supply gives a potential of 0.7–1.3 GtCO₂ yr⁻¹ for BE and 2.1–3.7 GtCO₂ yr⁻¹ for BECCS. Deploying afforestation over 67–115 Mha of abandoned cropland achieves net mitigation potentials of 0.8–1.4 GtCO₂ yr⁻¹. The potential of natural regrowth over all abandoned cropland areas (98–161 Mha) is 0.8–1.2 GtCO₂ yr⁻¹. Land requirements per GtCO₂ mitigated are summarized in Supplementary Table 2, and the mitigation potentials for each future scenario are shown in Supplementary Table 3. The individual CDR options and their combination into different scenarios are described in detail in the following sections.

Table 1 Energy potentials and net mitigation potentials of mitigation options on historical and future abandoned cropland.

| | Variable | PA | Non-PA |
|--|---------------|------|--------|
| Abandoned cropland, historical (AC) | | | |
| Bioenergy potentials [EJ yr ⁻¹] | | | |
| Primary | Rainfed | - | 19.28 |
| | Mixed | - | 25.29 |
| Final | Rainfed | - | 9.45 |
| | Mixed | - | 12.39 |
| Mitigation potentials [GtCO ₂ eq yr ⁻¹] | | | |
| | BE rainfed | - | 0.62 |
| | BECCS rainfed | - | 1.69 |
| | BE mixed | - | 0.72 |
| | BECCS mixed | - | 2.13 |
| | AF | - | 0.82 |
| | NR | 0.28 | 0.50 |
| Abandoned cropland, historical and future (AC + AC4) | | | |
| Bioenergy potentials [EJ yr ⁻¹] | | | |
| Primary | Rainfed | - | 28.42 |
| | Mixed | - | 37.31 |
| Final | Rainfed | - | 13.92 |
| | Mixed | - | 18.28 |
| Mitigation potentials [GtCO ₂ eq yr ⁻¹] | | | |
| | BE rainfed | - | 0.91 |
| | BECCS rainfed | - | 2.49 |
| | BE mixed | - | 1.07 |
| | BECCS mixed | - | 3.14 |
| | AF | - | 1.19 |
| | NR | 0.33 | 0.67 |
| Abandoned cropland, historical and future (AC + AC8) | | | |
| Bioenergy potentials [EJ yr ⁻¹] | | | |
| Primary | Rainfed | - | 33.31 |
| | Mixed | - | 43.70 |
| Final | Rainfed | - | 16.32 |
| | Mixed | - | 21.41 |
| Mitigation potentials [GtCO ₂ eq yr ⁻¹] | | | |
| | BE rainfed | - | 1.07 |
| | BECCS rainfed | - | 2.92 |
| | BE mixed | - | 1.25 |
| | BECCS mixed | - | 3.68 |
| | AF | - | 1.38 |
| | NR | 0.37 | 0.78 |

Results are shown for each individual land-based option: bioenergy (BE), BE with CCS (BECCS), afforestation (AF) and natural vegetation regrowth (NR); and abandoned cropland dataset (AC, AC4, and AC8). NR is the only option considered inside priority areas (PA) for biodiversity conservation. Results for each individual future scenarios (AC4 and AC8) are shown in Supplementary Table 3.

Natural regrowth. Reserving all cropland abandoned from 1992 to 2018 to natural vegetation regrowth can sequester up to 0.8 ± 0.08 GtCO₂ yr⁻¹ (Fig. 2a), which becomes 1.0 ± 0.11 GtCO₂ yr⁻¹ with AC4 and 1.2 ± 0.12 GtCO₂ yr⁻¹ with AC8 (Supplementary Fig. 3). The mitigation inside priority areas for biodiversity conservation is 0.3 ± 0.03 GtCO₂ yr⁻¹ (Fig. 2b). Average mitigation yields are 8.9 tCO₂ ha⁻¹ yr⁻¹ inside priority areas and 6.9 tCO₂ ha⁻¹ yr⁻¹ outside. Land within priority areas has a larger mitigation potential because they are usually located in the tropics, where vegetation growth rates are naturally high (Fig. 2b). On average, yields inside priority areas are about 30% higher than those outside, but in some cases, sequestration rates in the tropics can be an order of magnitude higher than those at mid or high latitudes. This is an important synergy between nature conservation and climate change mitigation. Tropical areas have

experienced large ecosystems degradation, but their high recovery potential is an attractive natural climate solution⁴⁸.

Afforestation. Net average mitigation potentials from afforestation of abandoned cropland outside biodiversity priority areas are 0.8 GtCO₂eq yr⁻¹ in historical abandoned cropland (Fig. 2c), 1.2 GtCO₂eq yr⁻¹ in AC + AC4, and 1.4 GtCO₂eq yr⁻¹ in AC + AC8 (Supplementary Fig. 4). Corresponding global average yields are 11.5 GtCO₂eq ha⁻¹ yr⁻¹, similar for all study areas. Life cycle emissions related to afforestation (0.8 – 1.2 MtCO₂eq yr⁻¹) are much smaller than its mitigation potential, thus having a negligible effect. The optimal distribution of forest types to the identified land areas is 45% to coniferous forests and 55% to non-coniferous forests (Supplementary Fig. 5a). Average yields are 7.5 tCO₂eq ha⁻¹ yr⁻¹ and 12.2 tCO₂eq ha⁻¹ yr⁻¹ for coniferous and non-coniferous forests, respectively. Non-coniferous forests include both deciduous and evergreen broadleaf forests, with the latter being highly productive in the tropical band. Coniferous forests typically have higher CO₂ sequestration potential in temperate and boreal climates. Afforestation yields are higher in the equatorial belt, where they can be up to 33 tCO₂eq ha⁻¹ yr⁻¹ (maximum yield, Southeast Asia), and they are about half of it in temperate regions (and even lower in boreal and mountainous climates).

The establishment of afforestation on recently abandoned cropland may require some land clearing, depending on the year at which the cropland was abandoned. The fate of this additional biomass, which is either immediately oxidized or used for bioenergy, influences the net climate change mitigation potentials of AF. These effects are estimated considering the amount of vegetation that accumulated on land since its abandonment, as well as the life-cycle emissions associated with land clearing and biomass conversion (if used for bioenergy). When biomass from land clearing is accounted for as an emission, the mitigation potentials from afforestation of abandoned cropland outside of priority areas is reduced by 0.4 GtCO₂eq yr⁻¹, resulting in a net mitigation of 0.4 , 0.8 , and 1.0 GtCO₂eq yr⁻¹ for AC, AC + AC4 and AC + AC8, respectively. This corresponds to a decrease in mitigation of 47%, 32 and 28%. When the biomass from land clearing is treated as an additional resource for bioenergy production, the mitigation potential increases by 0.6 GtCO₂eq yr⁻¹, leading to a new net mitigation of 1.4 , 1.8 , and 2.0 GtCO₂eq yr⁻¹ for AC, AC + AC4 and AC + AC8, respectively (a relative increase of 76%, 52 and 45%). See Supplementary Table 4 for a complete overview of the sensitivity analysis related to land clearing.

Bioenergy. Allocating all abandoned cropland outside priority areas to bioenergy production can achieve a mitigation potential that goes from 0.6 GtCO₂eq yr⁻¹ (AC, 67 Mha) to 1.1 GtCO₂eq yr⁻¹ (AC + AC8, 115 Mha) under rainfed conditions and from 0.7 GtCO₂eq yr⁻¹ to 1.3 GtCO₂eq yr⁻¹ under mixed water supply. Here, we assume that 50% of the biomass is used for production of 2G ethanol and 50% for FT diesel. When optimally distributed, global average crop yields are 381 GJ ha⁻¹ yr⁻¹, 151 GJ ha⁻¹ yr⁻¹ and 318 GJ ha⁻¹ yr⁻¹ with rainfed water supply for miscanthus, reed canary grass and switchgrass, respectively. By applying irrigation to bioenergy crops in areas not affected by water scarcity, there is an increase of 29%, 11 and 36% in crop productivity. Globally, miscanthus has higher yields than switchgrass and reed canary grass, but the latter two can better adapt to mid and high latitudes. The optimal feedstock distribution of rainfed crops on historical abandoned croplands outside biodiversity priority areas is 44% to miscanthus, 18% to reed canary grass and 38% to switchgrass (Supplementary

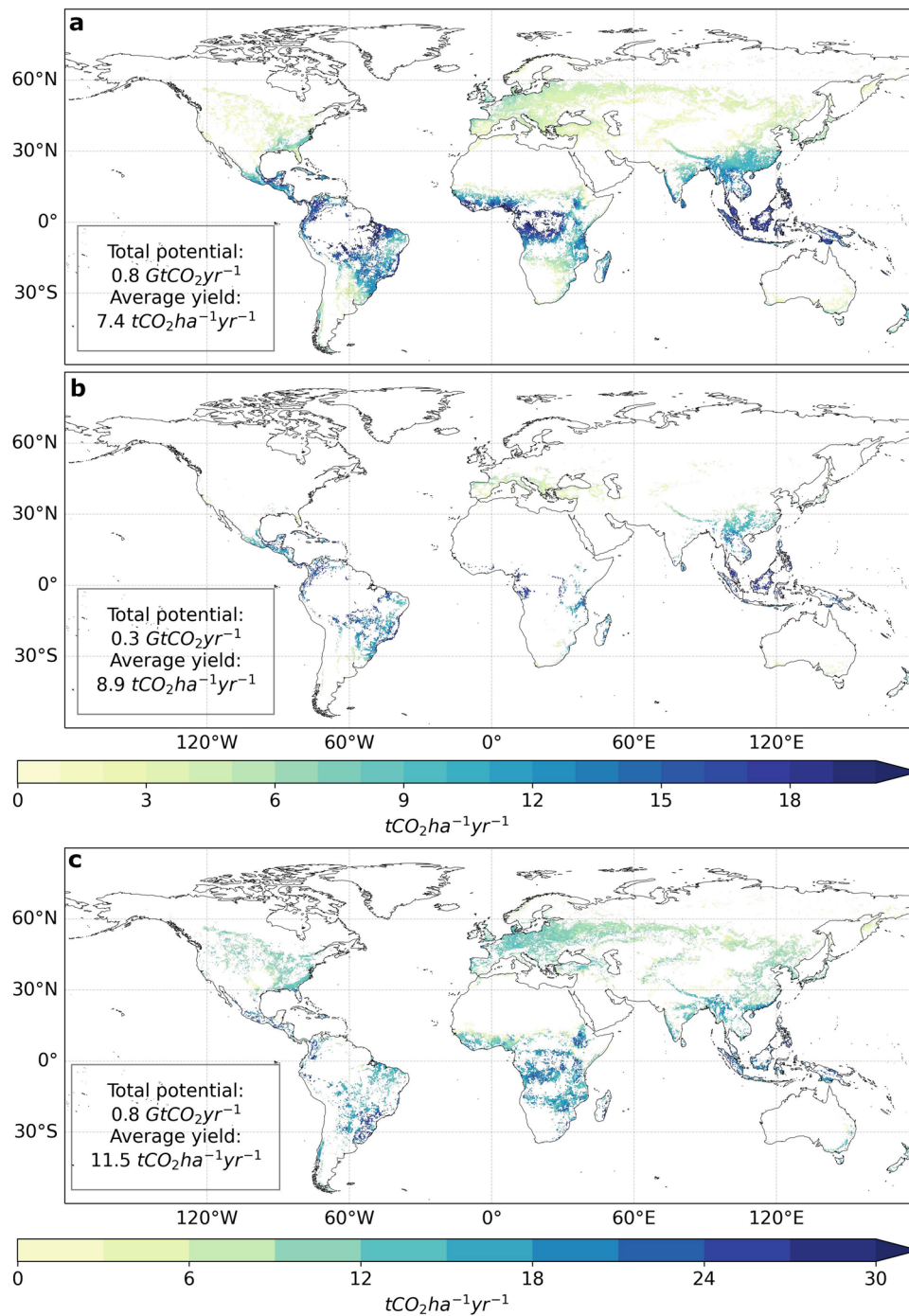


Fig. 2 Carbon sequestration potential of natural vegetation regrowth and afforestation on abandoned cropland. Natural regrowth yields in all historical abandoned cropland (AC) (a) and inside priority areas for biodiversity conservation only (b). Afforestation yields in abandoned cropland outside priority areas (c). Note differences between scales. Similar maps for AC4 and AC8 are shown in Supplementary Figs. 3 and 4.

Fig. 5b). The distribution is similar for mixed crops (Supplementary Fig. 5c) and for the future land availability scenarios.

In terms of primary energy potentials, rainfed-only crop production delivers 19–33 EJ yr⁻¹ and the mixed irrigation system 25–44 EJ yr⁻¹. The corresponding global average energy yields are 327 GJ ha⁻¹ yr⁻¹ (Fig. 3a) and 395 GJ ha⁻¹ yr⁻¹ (Fig. 3b). The increases in dry mass potential from rainfed to irrigated crops outside of both priority areas and water-scarce areas is 34% (Fig. 3c). See Supplementary Fig. 6 for yields of rainfed and mixed water supply crops in AC4 and AC8.

The highest biomass yields are found in the tropical band, in the east coast of the United States, and some parts of Europe. These areas are mainly located in tropical or temperate humid climates, where miscanthus and switchgrass are typically the dominant crop. Changing climatic conditions under RCP4.5 cause relatively small effects to bioenergy yields. For rainfed crops in the period 2011–2040 relative to 2041–2070, there is a global decrease in primary energy potential of 4% (Supplementary Fig. 7a). Around the equator, we mainly observe a decreasing potential. The largest increases occur in Central and East Asia. For mixed water supply, there is a global increase in primary

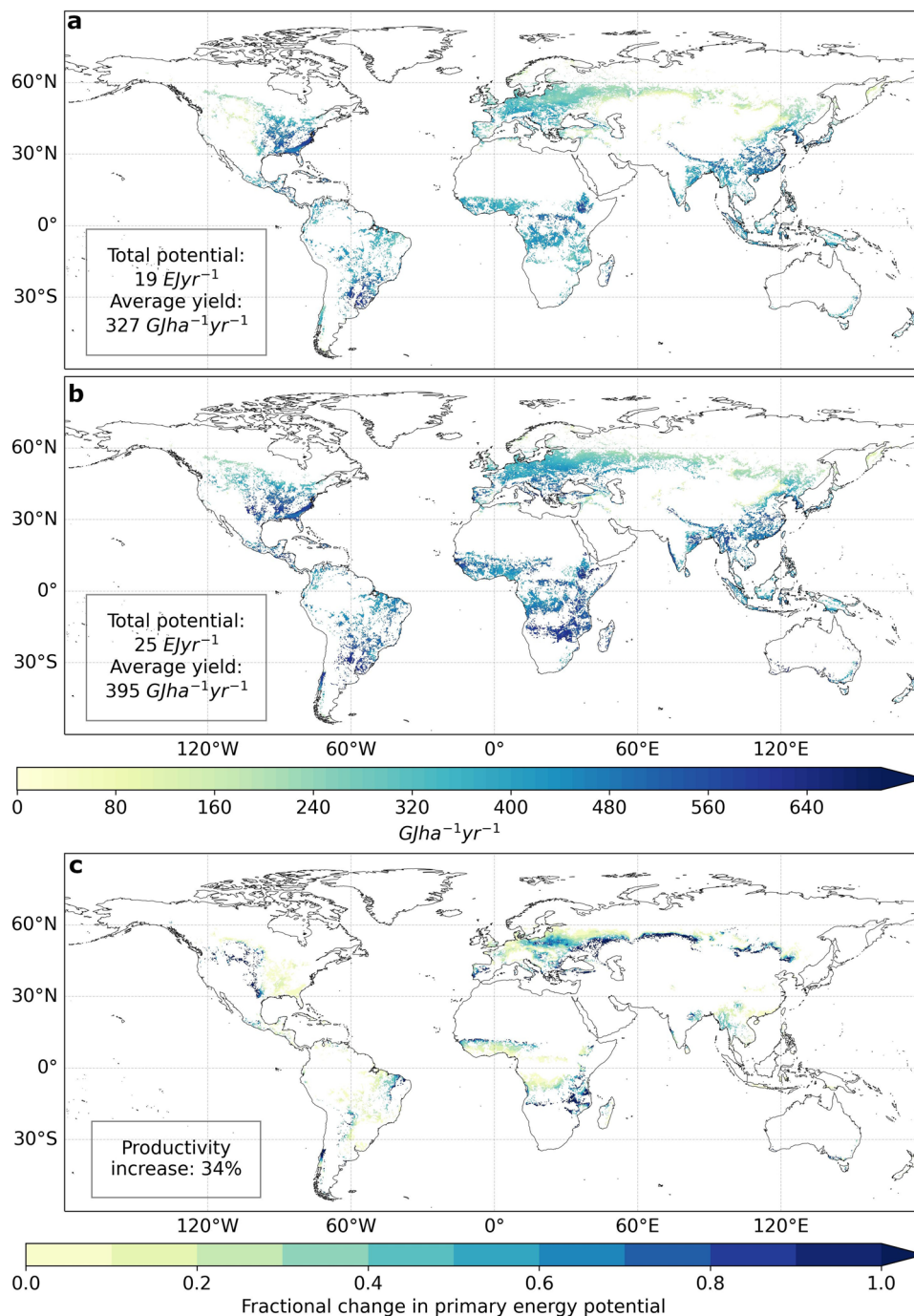


Fig. 3 Primary bioenergy yields on abandoned cropland outside priority areas for biodiversity conservation. Gridded bioenergy crop yields (optimal crop distribution) under rainfed conditions on historical abandoned cropland (AC) (**a**). Gridded bioenergy crop yields under mixed water supply conditions (rainfed within water-scarcity areas and irrigation outside) on historical abandoned cropland (AC) (**b**). Change in primary dry mass potentials between rainfed and irrigated crops in areas not affected by water scarcity (**c**). Similar maps for AC4 and AC8 are shown in Supplementary Fig. 6.

bioenergy potential of 2% (Supplementary Fig. 7b). This is because irrigation compensates for water deficits from heat waves or droughts during the crop growth cycle, securing yields from the adverse effects of climate change. Further, it can better support the positive effects of higher temperature and extended growing season on yields. The patterns around the equator are similar as for rainfed water supply, but with a lower decreasing potential. At latitudes above 30°N, there is an overall trend of increase in primary bioenergy potentials.

For rainfed BE, fossil fuel substitution can deliver a net climate change mitigation of 0.9–1.5 GtCO₂eq yr⁻¹, depending on the

land availability scenario (Fig. 4). About 55% of this mitigation comes from substituting fossil diesel with FT diesel, and the rest from 2G ethanol substituting gasoline. Life cycle emissions of biofuels production offset about one-third of the gross mitigation (0.3–0.5 GtCO₂eq yr⁻¹), and they are mostly associated with biomass production, especially when irrigation is applied. However, the higher life-cycle emissions from irrigation in areas of low water scarcity are compensated by the larger mitigation potential of higher yields. For example, the net mitigation potential of rainfed BE in the AC scenario is 0.6 GtCO₂eq yr⁻¹ (BE-rf). With irrigation (BE-mix), it becomes about 0.7 GtCO₂eq

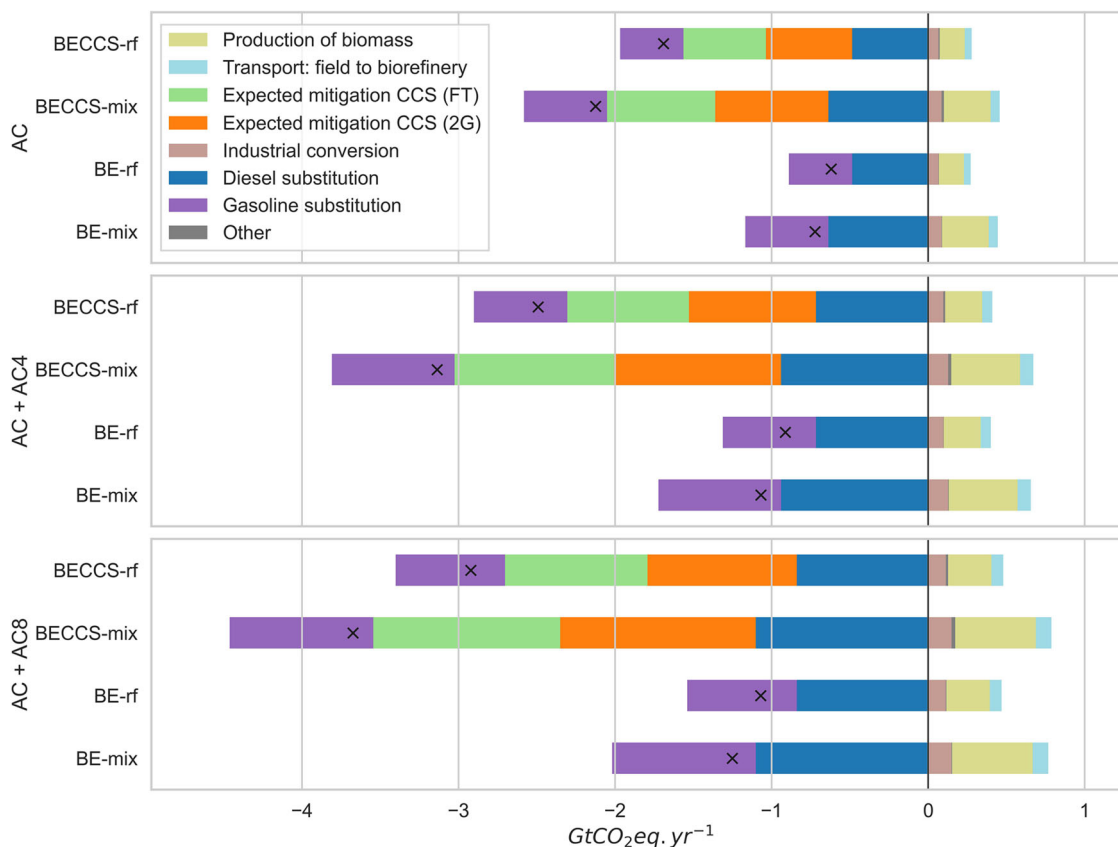


Fig. 4 Breakdown of the contributions to climate change mitigation potentials of bioenergy (BE) and bioenergy coupled with CCS (BECCS). Bioenergy crops produced under rainfed (rf) or mixed water supply systems (mix) on the investigated cropland abandoned scenarios (AC, AC4, and AC8). “Other” includes transport emissions from biorefinery to distribution for BE scenarios and additional emissions related to the energy penalty from the inclusion of CCS for BECCS scenarios. The symbol “x” inside the bars refers to the net mitigation of each scenario. Results for AC4 and AC8 scenarios are additive to those from AC (their individual contributions are shown in Supplementary Table 3).

yr^{-1} , that is $0.1 \text{ GtCO}_2\text{eq yr}^{-1}$ higher than rainfed conditions. This occurs because the increase in life-cycle emissions ($+0.2 \text{ GtCO}_2\text{eq yr}^{-1}$) is smaller than the increased mitigation potential from fossil fuel substitution from higher biomass yields ($+0.3 \text{ GtCO}_2\text{eq yr}^{-1}$).

The addition of CCS boosts the mitigation potentials at relatively low increases of life-cycle emissions. The net mitigation of BECCS from rainfed crops goes from $1.7 \text{ GtCO}_2\text{eq yr}^{-1}$ (AC) to $2.9 \text{ GtCO}_2\text{eq yr}^{-1}$ (AC + AC8), and from $2.1 \text{ GtCO}_2\text{eq yr}^{-1}$ (AC) to $3.7 \text{ GtCO}_2\text{eq yr}^{-1}$ (AC + AC8) with mixed water supply. About 55% of the mitigation comes from CCS, of which the largest share (51%) is from production of 2G ethanol (which has larger process emissions of CO_2 per MJ of fuel at the conversion plant than FT diesel). 2G ethanol also has higher life cycle emissions than FT diesel mostly due to the relatively high use of chemicals for biomass pretreatment and enzyme production.

As for afforestation, the net mitigation of BE and BECCS is affected by land clearing and the fate of the removed biomass. Depending on assumptions (Supplementary Table 4), mitigation potentials can either increase by $0.6 \text{ GtCO}_2\text{eq yr}^{-1}$ or decrease by $0.4 \text{ GtCO}_2\text{eq yr}^{-1}$. This results in a net mitigation increase of 58–100% and decrease of 36–62% for rainfed BE. For mixed BECCS, the potential increase in net mitigation is 17–29% and the corresponding decrease 10–18%.

Scenario analysis and optimal mitigation potentials. Allowing NR in all abandoned cropland has the potential of mitigating from $0.8 \pm 0.08 \text{ GtCO}_2\text{eq yr}^{-1}$ (AC) to $1.2 \pm 0.12 \text{ GtCO}_2\text{eq yr}^{-1}$ (AC + AC8) (Fig. 5), of which 36 and 32% is within priority areas.

Establishing forest plantations instead of NR outside priority areas (NR-AF scenario) increases the global climate change mitigation potentials to $1.1\text{--}1.8 \text{ GtCO}_2\text{eq yr}^{-1}$. This net mitigation is higher than what is achieved with the combination of NR and rainfed bioenergy production (NR-BE-rf), which is $0.9\text{--}1.4 \text{ GtCO}_2\text{eq yr}^{-1}$. The possibility to irrigate bioenergy crops in areas of low water scarcity (NR-BE-mix, $1.0\text{--}1.6 \text{ GtCO}_2\text{eq yr}^{-1}$) reduces the gap relative to NR-AF. To clearly outperform afforestation for climate change mitigation, bioenergy needs to be coupled with CCS. Between 2.0 and $3.3 \text{ GtCO}_2\text{eq yr}^{-1}$ can be achieved by adding CCS to rainfed bioenergy crops (NR-BECCS-rf), which become $2.4\text{--}4.1 \text{ GtCO}_2\text{eq yr}^{-1}$ when irrigation is added (NR-BECCS-mix).

Higher mitigation potentials are achieved when the spatial distribution of land-based options outside priority areas is allocated to the option that delivers the highest mitigation potential per individual grid cell. Given the influence of irrigation and CCS on the results, estimates are given both with and without these measures. With rainfed bioenergy crops without CCS, there is a global mitigation potential of $1.2\text{--}1.9 \text{ GtCO}_2\text{eq yr}^{-1}$. In addition to the land inside biodiversity priority areas that is dedicated to NR (31%), 15%, 7 and 48% of the abandoned cropland is allocated to BE-rf, NR and AF, respectively (Fig. 6a). With irrigated water supply in areas of low water scarcity, the global potential is $1.2\text{--}2.0 \text{ GtCO}_2\text{eq yr}^{-1}$, with the land outside priority areas distributed for 24% to BE-mix, 5% to NR and 41% to AF (Fig. 6b). Irrigation thus increases the land areas where BE can achieve larger benefits than AF, but forest plantations are still the best CDR option in most of the grid cells. When CCS is added to the system, the global mitigation potential is

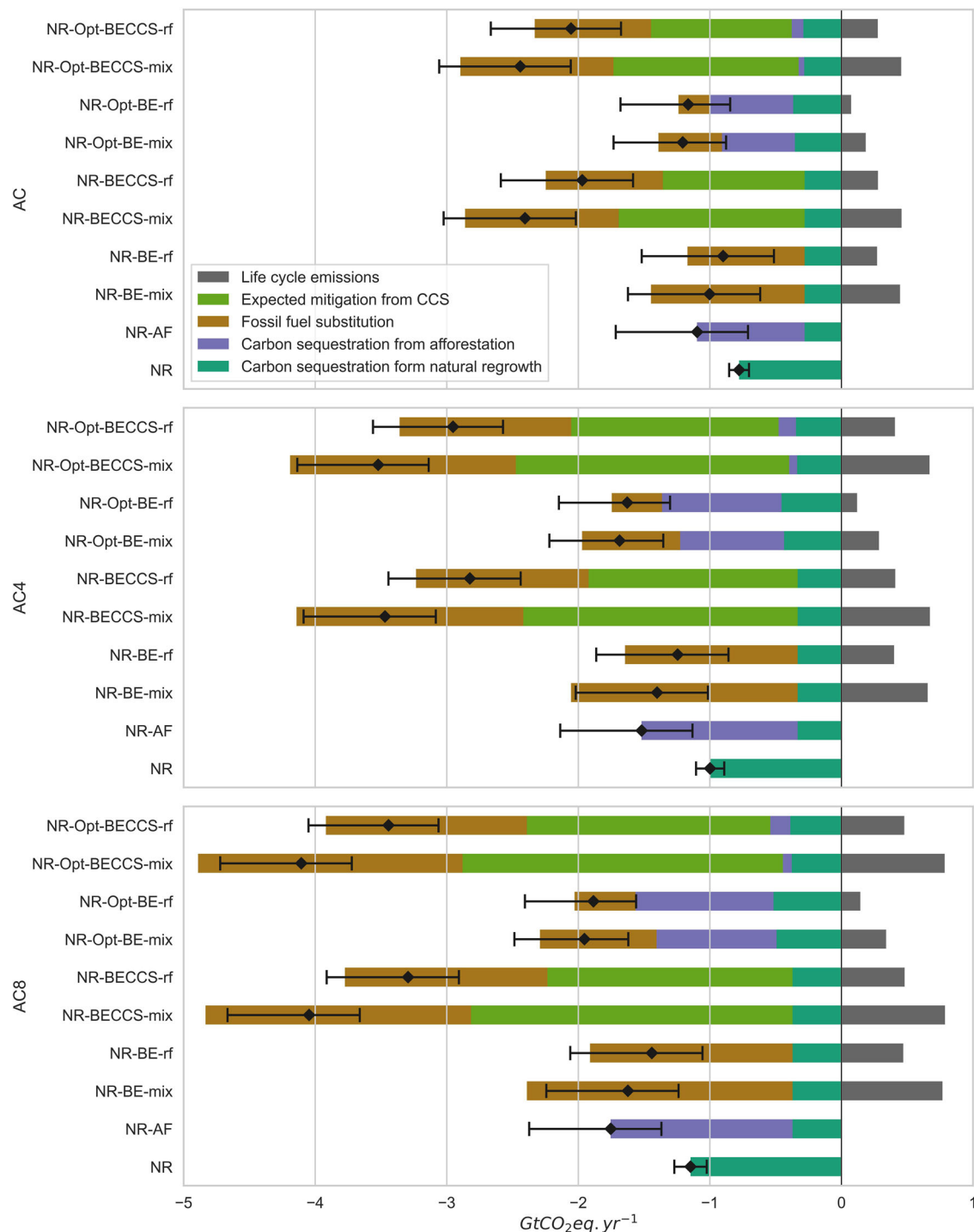


Fig. 5 Comparison of the climate change mitigation potentials of different combinations of land-based mitigation options on abandoned cropland.

Results are shown for different land availability scenarios (AC, AC4, and AC8) and water supply systems for bioenergy crops (rainfed: rf; irrigation in non-water scarcity areas: mix). Only NR is allowed within biodiversity priority areas. NR: natural vegetation regrowth; AF: afforestation; BE: bioenergy; BECCS: BE with CCS; Opt: optimal mitigation option considered (either with or without CCS and with or without irrigation). See Methods for a description of the scenarios. The uncertainty ranges refer to the possible contribution of aboveground biomass from land clearing (the diamond symbol indicates the net mitigation potential when land clearing is disregarded). The lower end of the range represents the case in which the biomass from land clearing is used as an additional source of bioenergy. The higher end is the case in which it is treated as an emission without energy recovery. For the NR scenario, the uncertainty range represents the ratio of model uncertainty relative to the best-fit model (one standard deviation).

2.1–3.4 $GtCO_2eq.yr^{-1}$, with an optimal distribution of CDR options of 53% to BECCS-rf, 3% to NR, and 13% to AF (Fig. 6c). By combining irrigation with CCS, the largest mitigation potential is achieved (2.4–4.1 $GtCO_2eq.yr^{-1}$) and BECCS clearly dominates the spatial distribution (Supplementary Fig. 8).

In general, NR is competitive or even better than AF in northern Sub-Saharan regions, around the Amazon basin, some areas in Southeast Asia and in southern Australia. Rainfed BE outperforms AF in the eastern half of the US, Southeast China and Central-Eastern Europe. Afforestation dominates at high

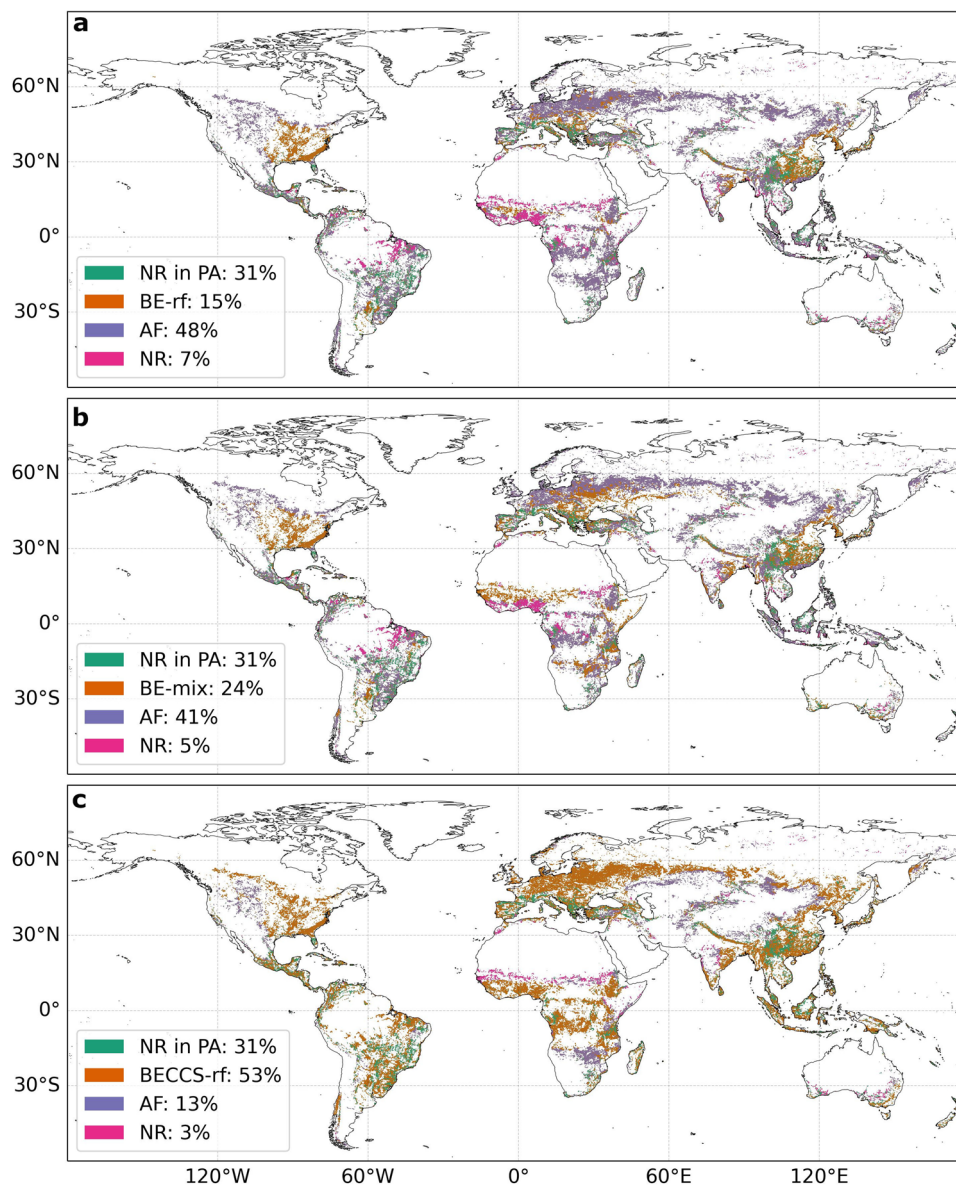


Fig. 6 Optimal distribution of mitigation options on abandoned cropland. Optimal combination of rainfed BE (BE-rf), NR and AF (**a**); rainfed and irrigated BE (BE-mix), NR and AF (**b**); rainfed BECCS (BECCS-rf), NR and AF (**c**). The boxes show the percentages allocated to each land-based option. For NR, the fractions outside and inside priority areas (PA) are indicated. NR is the only option considered within priority areas. Optimal combination of rainfed and irrigated BECCS (BECCS-mix), NR and AF are shown in Supplementary Fig. 8. Irrigation only occurs in areas not threatened by water scarcity. Due to equal spatial patterns for AC, AC4 and AC8, only maps for AC are shown.

latitudes and in the southern hemisphere. Irrigation and CCS clearly favor the potential of BE. When CCS is added, AF is stronger than BECCS in Western United States, and some areas in Southern Africa and Central Asia. NR remains competitive in a few locations only. Filtering average mitigation potentials per terrestrial ecoregion⁴⁹ shows that NR achieves the highest mitigation in tropical and subtropical forests, and the lowest in boreal and Mediterranean forests where temperature and water availability are a major constraint to natural vegetation growth (Supplementary Fig. 9). Afforestation is the superior mitigation option in tropical, subtropical, and boreal forests, and generally delivers higher mitigation than rain-fed bioenergy. In the other biomes, irrigated bioenergy can achieve higher yields, especially where water availability is a main limiting factor to crop growth, such as in dry and semi-arid climates (Mediterranean biomes, savannah, and shrublands). In all the other terrestrial ecoregions, the net mitigation potentials of AF and BE-mix are comparable.

Comparison with the literature. Although it is sometimes difficult to distinguish between definition of natural regrowth, afforestation, and reforestation in the different studies, our ranges of carbon sequestration from NR and AF are broadly consistent with those from other sources at regional levels. Reforestation, defined as the transition from <25 % forest cover to a >25 % forest cover, was found to potentially mitigate 10 GtCO₂eq yr⁻¹ in an area of 678 Mha⁶, corresponding to an average yield of 15 tCO₂eq ha⁻¹ yr⁻¹ (for comparison, NR in our study has a global average sequestration rate of 7.4 tCO₂eq ha⁻¹ yr⁻¹). This estimate covers a vast area, and it has already been identified as a likely overestimate⁷. Another study finds that natural regeneration of tropical secondary forests in Latin America could capture 31 GtC in 240 Mha of land in a period of 40 years⁵⁰, which corresponds to an average mitigation of 12 GtCO₂ ha⁻¹ yr⁻¹. Our study shows similar results, with NR yields ranging between 8 GtCO₂ ha⁻¹ yr⁻¹ and 18 GtCO₂ ha⁻¹ yr⁻¹ for the same region.

Previous estimates of mitigation potentials from afforestation show that a carbon sequestration of 0.5–5.1 GtCO₂eq yr⁻¹ can be obtained in 2050¹. An area of 320–970 Mha is required for a mitigation potential of 4.0–12.1 GtCO₂eq yr⁻¹ in 2100⁵¹ from afforestation and reforestation, which corresponds to a land requirement of 80 Mha per GtCO₂eq sequestered. Our results find that an average area of 83 Mha is required per GtCO₂eq sequestered through afforestation (Supplementary Table 2). Furthermore, a variety of global protection measures in forests and other ecosystems (which includes afforestation, reforestation, and land restoration) can mitigate 175 tCO₂eq ha⁻¹ from 2020 to 2050, corresponding to 6 tCO₂eq ha⁻¹ yr⁻¹. Our global average estimates are 6.8 tCO₂ ha⁻¹ yr⁻¹ from NR and 11.5 tCO₂eq ha⁻¹ yr⁻¹ for AF. Supplementary Fig. 10 compares future changes in forest cover estimated by SSP-RCP^{12–17} scenarios in 2050 with all abandoned cropland (historical and future) allocated to afforestation and NR in our study. Forest area changes in future scenarios vary widely, also when the same SSP or RCP is considered. In some cases, afforestation of abandoned cropland (AC + AC8) is sufficient to meet entirely (and beyond) the expected forest area expansion (e.g., in SSP4-RCP2.6). The minimum coverage (8%) is registered against SSP1-RCP2.6. In general, afforestation of abandoned cropland is a small share of the projected forest area expansion for SSP5 scenarios (especially under RCP2.6), as a large amount of negative emissions is required to offset GHG emissions from carbon-intensive sectors. The relative shares tend to be higher with SSP1, where more sector-wide mitigation measures reduce the demand for negative emissions.

A similar comparison can be performed with the estimates of BECCS in future scenarios. In 2050, global primary energy consumption is predicted to increase to 741 EJ yr⁻¹ (average of SSP1-4.5 and SSP2-4.5 across all models)^{12,15,17}, of which 71 EJ yr⁻¹ is bioenergy. Our results show a potential primary energy supply of 19–44 EJ yr⁻¹, which covers 27–62% of the average projected demand (Supplementary Fig. 11). In terms of land demand to grow second generation bioenergy crops, SSP estimates range between 150 Mha (SSP2-4.5) and 210 Mha (SSP1-4.5) in 2050². Our estimate of abandoned croplands is of 67–115 Mha (with the exclusion of biodiversity priority areas), representing 21–23% of future demands for bioenergy crops.

In our study, the mitigation potential from BECCS is up to 3.3 GtCO₂eq yr⁻¹. A BECCS median mitigation potential of 3 GtCO₂eq yr⁻¹ in 2050 is estimated for scenarios limiting global warming to less than 1.5 °C¹⁷. Other studies show similar results for the mitigation potentials, and identify a land area requirement for bioenergy crops of 31–58 Mha for each GtCO₂eq mitigated by BECCS⁵¹. Our analysis finds that 31–40 Mha of land is required to mitigate 1 GtCO₂eq yr⁻¹, depending on whether irrigation is included or not (Supplementary Table 2).

Limitations and uncertainties

Social, economic and political barriers affects all investigated options^{6,51,52}. NR is a cost-effective measure that is highly efficient in the tropics, but it requires a framework of enabling conditions (e.g., poverty alleviation, “food first” principle, land ownership rights, etc.) to be sustainably deployed⁵³. Effective governance, financial support, and international cooperation are of high importance for successful ecosystem recovery and climate change mitigation⁴⁸. Natural regeneration usually has the largest positive effects for biodiversity and habitat restoration⁵⁴, reducing the risks from introducing non-native species^{55,56}. Relative to cropland, forest plantations and perennial grasses grown for bioenergy also have positive effects for biodiversity, provided that a mix of native species are grown instead of monocultures^{30,57}. CCS is still facing techno-economic challenges for being

competitive in the market at current carbon taxes^{31,58}, and irrigation, even when deployed in non-water scarce areas, can require investments in costly infrastructure, which can represent a major barrier in developing countries^{59,60}.

Several uncertainties need to be considered when interpreting our results. Our study does not include soil organic carbon (SOC) changes, which are highly uncertain. Robust global datasets of SOC changes following natural revegetation, afforestation, or bioenergy crops are not currently available. Both positive and negative changes in soil and below ground carbon for NR and AF are reported, depending on multiple local factors and climatic conditions. On an average global scale, carbon accumulation in soils after NR is estimated negligible or negative in most biomes, but with large confidence intervals⁸. Using a low-confident global average estimate of 1.52 tCO₂ ha⁻¹ yr⁻¹ for the top 30 cm profile where most soil accumulation is expected to occur⁸, a total sequestration of 0.046 GtCO₂ yr⁻¹ over historical abandoned cropland within biodiversity priority areas (30 Mha) can be quantified. This represents 16% of the mitigation from above-ground vegetation (0.28 GtCO₂ yr⁻¹). Divergent responses to SOC are also found for afforestation^{61,62}. The mechanisms of soil carbon dynamics are still poorly understood, thereby limiting our capacity to quantify SOC changes from large-scale afforestation efforts. Existing meta-analyses generally conclude that SOC for natural or planted forests can either increase, decrease, or remain constant depending on multiple factors, such as tree species, local climate, soil type, land use history, etc.^{61,63}. Fixed ratios used to link biomass and soil carbon changes typically overestimate soil carbon enhancement of afforestation⁶¹. The afforestation model used in our study estimates a maximum accumulation rate of soil carbon of 0.15 tCO₂ ha⁻¹ yr⁻¹ for coniferous and 1.28 tCO₂ ha⁻¹ yr⁻¹ for deciduous forests⁶⁴. However, these factors are highly uncertain, as they are averaged globally and do not specify a soil depth. Their consideration in the analysis could add a mitigation of 0.010 GtCO₂ yr⁻¹ or 0.086 GtCO₂ yr⁻¹ on historical abandoned cropland outside of priority areas (67.4 Mha) for coniferous and deciduous forests, respectively. These estimates represent 2 and 10% of the AF mitigation potential in above-ground forest biomass (0.8 GtCO₂ yr⁻¹). A more consistent trend in SOC changes is observed for perennial grasses, which usually increase SOC at varying rates^{65–67}. A global meta-analysis estimated mean SOC changes (soil depth 0–100 cm) after the conversion of cropland to switchgrass or miscanthus at 5.9 and 3.3 tCO₂ ha⁻¹ yr⁻¹, respectively, but with 5th and 95th percentiles ranging from negative values (i.e., a SOC loss up to -7.33 tCO₂ ha⁻¹ yr⁻¹) to positive values up to three times the mean⁶⁷. Applying these mean factors to our analysis (and assuming for reed canary grass the same rate of miscanthus), we find that an average of 0.29 GtCO₂ yr⁻¹ can be sequestered in the soils in the BE-rf scenario on AC outside priority areas (for which we estimated a global mitigation potential of 0.62 GtCO₂ yr⁻¹). This means that our estimates of climate change mitigation potentials for BE and BECCS could be underestimated of about 30%. The underestimation will likely be representative for the first 10–15 years after the land use change, as soil sequestration rates significantly decline after 10 years for most land use types and transitions⁶⁷. Given the lack of robust global datasets and large variability of available estimates, we refrained from directly including in our analysis contributions from SOC changes.

The areas of abandoned cropland are derived using the land cover products from the European Space Agency Climate Change Initiative (ESA-CCI) and the Copernicus Climate Change Service (C3S-CDS). Several previous studies have validated and assessed their accuracy (see Methods)^{21,68–70}. The improvements relative to other global land cover datasets are significant, as well as their robustness in assessing changes in cropland extent, but some

limitations remain, mainly due to potential misclassifications. The global overall accuracy is 71%, but it varies with spatial location and between classes. Compared to other land cover products, the identified abandoned cropland with ESA-CCI and C3S-CDS data are usually found to be conservative^{2,71–73}.

Future locations of abandoned cropland are highly uncertain and scenario dependent, and previous studies highlighted that inter-model differences can be larger for the same SSP than between different SSPs⁷⁴. Hence our selection of a simple and transparent approach where future abandoned cropland has a high probability to occur on cropland nearby previously abandoned land. To explore the sensitivity of our results to the land use scenario, we re-run the analysis using alternative land use projections that have similar extension of cropland abandonment. These projections are consistent with the SSP-RCP framework and are produced by downscaling the outputs from the Integrated Assessment Model (IAM) GCAM⁴⁵. Among the available scenarios, SSP2-RCP4.5 has a total abandoned cropland area by 2050 that is the closest to AC4 (both around 41 Mha), and SSP4-RCP6.0 (84 Mha) to AC8 (63 Mha). A comparison of the spatial patterns of these alternative scenarios are shown in Supplementary Fig. 2, while their mitigation potentials are summarized in Supplementary Table 5 and Fig. 12. As expected, the maps tend to diverge in both intensity and locations of abandoned cropland. However, the mitigation potentials are largely consistent for the scenarios with similar total identified land. The average change in climate change mitigation potential estimates is $-0.04 \text{ GtCO}_2\text{eq. yr}^{-1}$ for AC4-SSP2-RCP4.5 (about -9% of the average potential across land-based options) and $0.09 \text{ GtCO}_2\text{eq. yr}^{-1}$ for AC8-SSP4-RCP6.0 (about 10% of the average potential across land-based options). Despite the variability in the spatial patterns of the datasets, as long as they have similar total areas and abandoned land is distributed at global scales within existing cropland areas, results are largely consistent and insensitive to the individual scenario.

There are uncertainties related to the estimates of carbon sequestration rates from NR, AF, and bioenergy crop yields, which are discussed in detail in a text in the Supplementary Information. Maps of NR rates are gathered from a study that applied a machine learning algorithm to more than 13,000 georeferenced measurements of carbon accumulation⁸. The grid-specific error ratios (reproduced in Supplementary Fig. 13 for AC) were used to explore the variability in our results, with the corresponding range around mean values shown in Fig. 5. Afforestation scenarios rely on the Global Forest Model (G4M)^{75,76}, a well-established model linked to the IAMs GLOBIO and MESSAGE for estimating land use change and forestry emissions for a set of SSP-RCP scenarios^{77–79}. The model is based on satellite retrievals of net primary production and data provided by the Global Forest Resources Assessment (see Methods), and tested against observations and in multi-model inter-comparison studies^{80–82}. Bioenergy crop yields are produced from the model Global Agro-Ecological Zones version 4 (GAEZv.4) (see Methods). When compared to observations (Supplementary Fig. 14), GAEZv.4 tends to underestimate miscanthus yields, overestimates switchgrass yields, and has relatively better accuracy in reproducing yields of reed canary grass. In many cases, the uncertainty range of the predictions and observations overlap, indicating that the model can generally capture the variability in the observed yields. In our study, the over- and under-estimate of the yields tend to compensate at a global total, as the optimal allocation of crop types per grid cells attributes 44% of the land to miscanthus and 38% to switchgrass (Supplementary Fig. 5b). The accuracy of the predictions from GAEZv.4 is in line with those of other frequently used bioenergy yield models (Supplementary Table 6). If we use another

observationally-constrained model⁸³ to estimate bioenergy potentials, there is a global average reduction in yields relative to GAEZv.4 of $3.14 \pm 4.63 \text{ t ha}^{-1} \text{ yr}^{-1}$, an RMSE of 5.59, and a correlation between the two datasets of 0.902 ($p < 0.01$) (Supplementary Fig. 15). At a global level, GAEZv.4 predicts a total amount of rainfed bioenergy crops from AC of 1.05 Gt yr^{-1} , against 0.87 Gt yr^{-1} estimated from the alternative yield model. This is a variability of 17%, which falls within the uncertainty ranges in Fig. 5 (where the mitigation potential from rainfed bioenergy crops varies of about 40% around the mean). The main difference between the models is that GAEZv.4 is a parametric model and yields reflect optimal and commercially oriented management, while the other is extrapolated from observed yields, which typically fluctuate with varying management practices and objectives across field studies. Overall, GAEZv.4 can reproduce observed yields and its performances are comparable to other models, so the use of another global model does not substantially affect the main conclusions of our study.

Final remarks

The urgency of the climate crisis calls for simultaneous deployment of multiple mitigation strategies to constrain global warming. Land-based mitigation options are not a substitute for reducing fossil fuel emissions, but rather an essential complement that, in the case of bioenergy production, they also help to phase out fossil fuels. Due to the reduced direct costs, regrowth of natural vegetation on abandoned cropland is the measure with the largest potential co-benefits with nature conservation. However, this study shows that selective afforestation can improve the carbon sequestration potential in many locations around the globe. Tree planting should be carefully planned considering local environmental conditions to avoid negative side-effects, such as increased risks for biodiversity or soil desiccation by using non-native species. On the other hand, natural vegetation restoration is more cost-effective and prevents the negative biodiversity outcomes of tree establishment on native grassland. Investments in infrastructure, transformative changes, and technological progress are required to achieve larger mitigation potentials through bioenergy and CCS and get closer to the levels indicated by future stringent climate change mitigation scenarios. The use of abandoned cropland can mitigate trade-offs because this land has been usually degraded from its natural state by farming activities, it is typically located near roads, and it requires less site preparation. Specific policies are required to secure the use of abandoned cropland for mitigation purposes, and prevent risks of reclamation for food production as sometimes observed in the recent past⁸⁴.

Our results help to understand the relative performances of different land-based mitigation options per hectare of land across the globe and for terrestrial ecoregions, but their implementation should consider the local environmental and social context, as all options require political will and financial resources. The latter are to be considered alongside other important feasibility criteria, such as costs, livelihoods, and social suitability. Aspects connected to the permanency of the carbon storage, saturation of the carbon sink, energy security, and socio-economic factors are key elements in a multi-criteria analysis together with climate change mitigation and nature conservation. Meeting the projected CDR demand in low-temperature target scenarios requires land areas beyond what is currently available from abandoned cropland. Stronger reduction in the demand for food and feed products through sustainable agriculture intensification and dietary changes are needed to minimize the adverse side-effects for food security and the environment. Cross-sectoral and integrated policies are essential to harmonize multiple drivers of land use

changes and identify the strategies to address the most relevant global challenges in each given regional context by merging environmental and socio-economic factors.

Methods

Historical cropland abandonment (AC). Recent efforts have made available improved datasets of historical abandoned cropland at various temporal and spatial scales, from regional to global⁸⁵. Time-series of high-resolution satellite data of 37 land cover classes across the globe are distributed by the European Space Agency Climate Change Initiative (ESA-CCI)⁸⁶. These land cover products have a 300 meters (or 10 arc seconds) horizontal resolution at the equator and are obtained by combining several earth observation products and by using the GlobCover unsupervised classification chain. Recent studies used these data to identify abandoned croplands from 1992 to 2015^{21,44}. The Copernicus Climate Change Service climate data store (C3S-CDS) further released land cover maps from 2016 to present that are consistent with the ESA-CCI dataset^{43,87}. Here, we integrate the two datasets and extend the identification of cropland abandonment to 2018. The two land cover products are highly consistent, with the same spatial resolution and temporal scale²⁶. Validation efforts show that they are among the most accurate global products in the identification of cropland areas⁸⁶. Global user and producer accuracy values for cropland classes are in the range of 85–94% for the ESA-CCI products and 76–92% for the C3S-CDS products, with medians of 89 and 82%, respectively^{42,88}. Regional overall accuracies are between 70 and 84% in South America, China, and Eurasia, and lower than 65% in Africa and the Arctic²⁶.

The analysis is conducted at a grid-cell level at 10 arc seconds resolution, and abandoned cropland is identified by selecting the grid-cells classified as cropland classes in 1992 but not in 2018. Cropland translated to urban settlements is excluded. The resolution is further up scaled to 30 arc seconds (for consistency with the natural regrowth data) and then to 5 arc minutes (to match bioenergy and afforestation data).

Future cropland abandonment (AC4 and AC8). Cropland abandonment is a process that is also expected to continue in the future⁸⁹. The most sustainable SSPs predict dietary changes and increasing efficiency in food systems and agriculture that can decrease pressure on land^{5,90}. However, spatial patterns of future abandoned cropland are inherently uncertain, and projections are highly diverging even for the same SSP scenario^{74,91–93}. We apply a simple and transparent method to estimate future areas of abandoned cropland. The rationale is that cropland abandonment is a dynamic process rooted in regional socio-economic contexts^{94–96}, and new cropland abandonment has higher probability to occur near areas that have been already abandoned⁸⁴. The nearest neighbor method is used to identify areas of future abandoned croplands within a maximum of four or eight nearby cells. If one of the cells nearby a historically abandoned cropland cell is currently cropland, it is changed into abandoned cropland. This generates two land availability scenarios (See Supplementary Fig. 16 for a simplified visualization), which are spatially consistent with the historical trend. In our study, there are thus three cases of land availability: AC (historically abandoned cropland area from 1992 to 2018), AC4 (future abandoned cropland identified with a maximum of four cell extension) and AC8 (future abandoned cropland identified with a maximum of eight cell extension).

Our future land use scenarios are compared with those of the SSP-RCP framework produced by downscaling the outputs from the Integrated Assessment Model GCAM⁴⁵. From all the available scenarios, we identified the areas of cropland abandoned by tracking cell-specific fractional cropland contraction over time (cropland that transitioned to human settlements was excluded). A generic cropland class was produced by aggregating all crop-based land types from 15 to 28. From all the available scenarios, we identified the areas of cropland abandoned by 2050 following the same approach used for the historical dataset. We then selected SSP2-RCP4.5, which has a similar area of AC4 (41 Mha), and SSP4-RCP6.0 (84 Mha), which is the closest to AC8 (63 Mha). The spatial patterns of these alternative scenarios are shown in Supplementary Fig. 2, and the corresponding results in Supplementary Table 5 and Fig. 12.

Biodiversity priority areas and water scarcity. Ensuring that the highest-ranked areas for biodiversity are preserved for nature conservation greatly contributes to achieve global species conservation targets, while at the same time contributing to climate change mitigation by increasing carbon storage in the restored vegetation. To integrate these two strategies, we use a recently produced dataset of priority areas⁷ that ranks global regions after their need for biodiversity conservation via a multicriterial optimization approach that identifies priority areas for restoration across all terrestrial biomes. Restoring 15% of converted lands globally (consistent with Aichi Biodiversity Target 15) could reduce the current global extinction debt by 63 ± 4% if concentrated in priority areas for biodiversity⁷. The identified priority areas largely overlap with previously mapped biodiversity hotspots⁹⁷ and other conservation areas⁹⁸ (see Supplementary Fig. 17a). We, therefore, considered that if abandoned cropland falls within the 15% of the priority areas for biodiversity conservation, NR is the only CDR measure allowed. In other words, AF, BE and BECCS can only occur in the abandoned cropland that is not located within the 15% of the priority areas for conservation.

Given the large increase in bioenergy crop yields that can be achieved with irrigation relative to rain-fed growing conditions^{21,59}, and the risks for increased water depletion of irrigation⁹⁹, our analysis considers both types of water supply systems. As sustainable water withdrawals are already a concern related to large-scale agricultural practices and future bioenergy potentials^{34,59,60}, we introduced a layer of water scarcity based on the map from AQUASTAT and the Food and Agriculture Organization (FAO)¹⁰⁰ in the scenarios assessing potentials from irrigated bioenergy crops. In this dataset, global land areas are grouped into three categories of low, moderate and high water scarcity. Areas characterized by moderate and high water scarcity are those where water use is 10–20% and >20% of renewable water resources, respectively. The spatial distribution of areas of high and moderate water scarcity is shown in Supplementary Fig. 17b. In our analysis, BE and BECCS can only be irrigated outside areas of moderate and high water scarcity, wherein only rainfed water supply occurs.

Land-based mitigation scenarios. The different CDR options (NR, BECCS, and AF) and BE are combined in 10 scenarios for each of the land use dataset, i.e., the historical (AC) and the two future projections (AC4 and AC8). We evaluate the period until 2050. The scenarios are the following:

- NR-BE-rf: Natural regrowth within biodiversity priority areas. Rainfed bioenergy production outside priority areas.
- NR-BECCS-rf: Natural regrowth within biodiversity priority areas. Rainfed bioenergy production with CCS outside priority areas.
- NR-BE-mix: Natural regrowth within biodiversity priority areas. Outside priority areas, rainfed bioenergy production in water-scarce areas and irrigated bioenergy production outside water-scarce areas.
- NR-BECCS-mix: Natural regrowth within biodiversity priority areas. Outside priority areas, rainfed bioenergy production with CCS in water-scarce areas and irrigated bioenergy production with CCS outside water-scarce areas.
- NR-AF: Natural regrowth within biodiversity priority areas. Afforestation outside priority areas.
- NR-all: Natural regrowth in all abandoned cropland.
- NR-Opt-BE-rf: Natural regrowth within biodiversity priority areas. Outside priority areas, optimal distribution (i.e., higher mitigation achieved) among rainfed bioenergy production, natural regrowth, and afforestation.
- NR-Opt-BECCS-rf: Natural regrowth within biodiversity priority areas. Outside priority areas, optimal distribution among rainfed bioenergy production with CCS, natural regrowth, and afforestation.
- NR-Opt-BE-mix: Natural regrowth within biodiversity priority areas. Outside priority areas, optimal distribution among bioenergy production, natural regrowth, and afforestation outside priority areas. Rainfed water supply for bioenergy crops in water-scarce areas and irrigated outside.
- NR-Opt-BECCS-mix: Natural regrowth within biodiversity priority areas. Outside priority areas, optimal distribution among bioenergy production with CCS, natural regrowth, and afforestation outside priority areas. Rainfed water supply for bioenergy crops in water-scarce areas and irrigated outside.

Natural regrowth is the only mitigation strategy inside priority areas for biodiversity conservation in all scenarios. This means that the results presented for BE, BECCS, and AF consider only areas outside of the biodiversity priority areas. The term “Opt” refers to the optimal allocation to each grid-cell of either BE (or BECCS), NR and AF, according to the option that delivers the largest mitigation potential.

Natural vegetation regrowth. A spatially explicit dataset of 30 arc seconds resolution⁸ is used for estimation of carbon sequestration due to natural vegetation regrowth. The natural regrowth data are presented as the potential carbon sequestration from passive recovery to forest and savanna biomes with a >25% forest cover. Calculations of natural regrowth in abandoned cropland are conducted at 30 arc seconds resolution and further up scaled to 5 arc minutes resolution for consistency with the rest of the data. The natural regrowth data are based on historical data from 257 studies and 13,112 georeferenced measurements of carbon accumulation. As climatic factors explain variation in rates better than land-use history, the field measurements were combined with 66 environmental covariate layers to create a global map of potential aboveground carbon accumulation rates for 30 years of natural forest regrowth. The ensemble model had a residual mean square error (RMSE) of 0.798 t C ha⁻¹ yr⁻¹ and an R² of 0.445 on the independent test set. More information about the model and its validation are available in Supplementary Note 1 (“Natural regrowth”). Aboveground biomass includes stem and branch biomass. This map has over 100-fold variations in rates across the globe and shows that IPCC default rates generally underestimate aboveground carbon accumulation by 32% on average⁸. This dataset is used to estimate the climate change mitigation potential of NR on historical and future abandoned cropland. For each grid cell, both average sequestration rates and reported standard deviations are used.

The natural regrowth data are also used to estimate the amount of dry mass or carbon that accumulated on abandoned cropland from 1992 before the establishment of either perennial grasses or forest plantations. Recent studies have

combined natural regrowth data and satellite observations to estimate historical accumulation of carbon on abandoned cropland for specific regions^{84,101}, and here we provide the first global assessment. As the fate of this carbon is uncertain (it can either be used for bioenergy or rapidly return to the atmosphere), the effect that the carbon costs of land clearing can have on the net climate change mitigation potentials of each CDR option is explored in a sensitivity analysis. If used for bioenergy production, biomass from land clearing is assumed to have average characteristics in terms of carbon content and lower heating value of several types of forest/wood residues (Supplementary Table 7). The corresponding life-cycle emissions of biomass harvesting to clear the land and convert it into biofuels are included in the analysis. When abandoned cropland is allocated to natural vegetation regrowth, the aboveground biomass is left for continued growth.

Afforestation. With afforestation, we refer to the artificial establishment of selected regional established tree species and implementation of sustainable silvicultural practices to enhance carbon sequestration relative to natural forest regrowth. Mitigation potentials of afforestation are estimated with the Global Forest Model (G4M)^{76,102,103}. G4M uses biomass data from FAO, yield tables and MODIS NPP to parameterize increment functions, together with information on local soil characteristics, temperature and precipitation¹⁰². Forest management includes activities such as selection of optimal tree species group, rotation period, and thinning intensity⁷⁷. The model has been widely used in the international scientific community^{77,78,81,104,105} and is coupled to the integrated assessment model MESSAGE and the land-based economic model GLOBIOM⁷⁹ (by which it was used for estimating forestry emissions for a set of SSP/RCP scenarios). Afforestation dynamics are estimated for each grid cell based on local environmental conditions⁶⁴, and can be simulated for different background climates⁷⁶. More information on the validation and applications of G4M are available in Supplementary Note 1 (“Afforestation”).

We quantified afforestation potentials using G4M driven by SSP2-RCP4.5 multi-ensemble mean climate data from the EC-Earth3 model¹⁰⁶. Mean annual increment ($\text{tC ha}^{-1} \text{yr}^{-1}$) was used to calculate the 30-year average carbon sequestration potential until 2050. Mean annual increment describes yield level and is proportional to the ratio between total stem wood carbon production per hectare and increment optimal harvest time. Increment is age-dependent and will vary according to e.g., climate, species and stand density⁷⁵. G4M simulates afforestation data of both coniferous and non-coniferous forests based on local site-fertility factors and climatic conditions⁷⁵. The optimal forest distribution between the two forest types is found by identifying the highest carbon sequestration potential in each grid cell. This optimal forest distribution is used for all scenarios involving AF.

G4M only simulates aboveground stem biomass. To account for the whole carbon content of the forest system (e.g., branches and roots), a default standard factor of 20% of extra biomass is added to the carbon content of each grid¹⁰⁷. This factor is tree and age dependent, and decreases with forest age, when the stem biomass becomes a larger part of the total aboveground biomass. Higher values are sometimes used, e.g., up to 40% in Refs. ^{108,109}. However, our analysis focuses on the first decades of forest establishment, and 20% represents a conservative estimate to prevent overestimations. Emissions from silvicultural activities are $0.3 \text{ tCO}_2\text{eq ha}^{-1}$ ¹¹⁰, and are one-time emissions occurring when the forest plantation is established.

Bioenergy crops. Bioenergy potentials are considered for three common types of perennial grasses that are harvested once a year: miscanthus, reed canary grass and switchgrass. Miscanthus is a C4 grass that grows native from tropic to sub-arctic regions¹¹¹. Reed canary grass is a C3 grass that thrives in cold climates and it is typically harvested in spring for optimal quality^{112,113}. Switchgrass is a C4 grass that grows native in North America and Europe¹¹⁴. These perennial grasses have shown promising properties as bioenergy feedstocks in test trials and their cultivation is expected to significantly increase in most future climate change mitigation scenarios⁵.

Yields of perennial grasses are estimated using the model Global Agro-Ecological Zones version 4 (GAEZv.4)¹¹⁵ with net calorific values (in MJ kg^{-1}) for miscanthus, reed canary grass, and switchgrass from the Phyllis2 Database¹¹⁶. Agro-climatic yields for miscanthus, reed canary grass and switchgrass are collected at 5 arc minutes spatial resolution. Several constraints are accounted for when producing the yield estimates, such as local temperature, moisture, and leaf area index, as well as risks of pests and diseases. In our analysis, we estimate grid-specific bioenergy potentials as the 30-year average for the period 2021–2050 under RCP4.5 climatic conditions (according to the HadGEM2-ES climatic model), high management intensity levels (i.e., market-oriented farming systems, highly mechanized with low labor intensity and with pest and disease control), and under both rainfed and irrigated water supply. Water requirements are calculated for all crop types and corresponding yield reductions are dependent on actual crop evapotranspiration and maximum crop evapotranspiration. GAEZv.4 uses irrigation to avoid yield losses from water stress by preventing crop water deficits during the growth cycle (so that crop water losses from evapotranspiration do not exceed absorption). A validation of GAEZv.4 yields against observations and other crop yield models are available in Supplementary Note 1 (“Bioenergy crop yields”).

The BE and BECCS scenarios rely on an optimal combination of miscanthus, reed canary grass, and switchgrass, which is found by identifying the grass with highest dry mass yield in each grid cell (Supplementary Fig. 5b, c).

Final energy production, CCS, and life cycle emissions. Perennial grasses are assumed to be used to produce second-generation (2G) ethanol and Fischer-Tropsch (FT) diesel, in equal shares. These are two common types of biofuels expected to be produced in the future for climate change mitigation in the transport sector¹¹⁷, and are representative examples of a biochemical (2G ethanol) and thermochemical (FT diesel) production route. Life cycle inventory data to produce biofuels are summarized in Supplementary Table 8. Cultivation of perennial grasses includes the major farming activities (soil preparation, fertilization, harvesting) and are specific to each type of perennial grass¹¹⁸. Nitrogen (N), phosphorus (P) and potassium (K) fertilizer application rates are site-specific, and they are equal to the nutrient contents of the harvested biomass plus losses due to volatilization and leaching, soil erosion rates and plant uptake inefficiencies¹¹⁸. Farming the mix of perennial grasses in our scenarios results in weighted average climate change impacts of 151 and 220 $\text{kg CO}_2\text{eq per ton(dry)}$ biomass for rainfed and irrigated crops^{119,120}, respectively. An average transport distance of biomass from field to biorefinery of 200 km is assumed at an average biomass moisture content of 17.5%¹²¹ (with emission factor of $0.171 \text{ kg CO}_2 \text{ per t-km}^{122}$). Emissions from industrial conversion of biomass to biofuels are assumed as 115 $\text{kg CO}_2\text{eq per ton(dry)}$ biomass^{121–123} for 2 G ethanol and 8.3 $\text{kg CO}_2\text{eq per ton(dry)}$ biomass¹²⁴ for FT diesel. Plant efficiency is 45% for production of 2 G ethanol¹²¹ and 53% for FT diesel¹²⁴, which means that 23 and 27% of primary bioenergy potential become final energy potential in terms of 2 G ethanol and FT diesel, respectively. CO_2 emissions at the biofuel conversion facility available for CCS are $0.160 \text{ kg CO}_2\text{eq MJ}^{-1}$ ¹²¹ from ethanol production and $0.138 \text{ kg CO}_2\text{eq MJ}^{-1}$ ¹²⁴ for FT diesel. Negative emissions from the CCS technologies are $-1046 \text{ kg CO}_2\text{eq per ton(dry)}$ processed biomass¹²¹ for 2 G ethanol and $-999 \text{ kg CO}_2\text{eq per ton(dry)}$ processed biomass¹²⁴ for FT diesel. These numbers are obtained after the inclusion of life cycle emissions for the CCS technology inputs (e.g., chemicals and energy inputs) ($0.004 \text{ kg CO}_2\text{eq per kg CO}_2$ sequestered)¹²⁵ and a carbon capture efficiency of 90%¹²⁵ of the carbon dioxide that would be vented out from industrial processes in the plant. We assume that all CO_2 emissions from industrial processes are available for capturing (both emissions from the gasification plant and from the heat and power generation area). The energy penalty for introducing CCS to the biorefinery system is 4.4% for 2G ethanol and 3.4% for FT diesel³¹, and it is modeled by an additional biomass consumption (and associated life-cycle emissions). Transport emissions from biorefinery to distribution are assumed for an average distance of 100 km ($5.1 \text{ kg CO}_2\text{eq per ton(dry)}$ processed biomass^{121,126} for 2G ethanol and $3.2 \text{ kg CO}_2\text{eq per ton(dry)}$ processed biomass¹²⁴ for FT diesel).

To estimate climate change mitigation potentials from replacement of gasoline (2G ethanol) and diesel (FT diesel), life cycle emissions of fossil fuels are assumed as $95.1 \text{ g CO}_2\text{eq MJ}^{-1}$ and $93.3 \text{ g CO}_2\text{eq MJ}^{-1}$ for diesel and gasoline, respectively. The final bioenergy potential (in GJ yr^{-1}) corresponds to the possible reduction in fossil fuels and the resulting mitigation potential. The analysis accounts for the emission of the three most important GHGs (CO_2 , N_2O , and CH_4), whose impacts are converted to CO_2 -equivalents using the Global Warming Potential for a time horizon of 100 years (GWP100).

Data availability

Data used in this study are publicly available from the references provided in the paper. Abandoned cropland data (for scenario AC, AC + AC4, and AC + AC8), G4M data, and natural regrowth data in historical abandoned cropland are made available at <https://doi.org/10.6084/m9.figshare.21901962>. Other data necessary to replicate the results can be collected from the following repositories: natural regrowth data from <https://data.globalforestwatch.org/documents/carbon-accumulation-potential-from-natural-forest-regrowth-in-reforestable-areas/about> (carbon accumulation potential) and <https://data.globalforestwatch.org/documents/d28470313b8e443aa90d5cbcd0f74163/about> (uncertainty ranges), biomass yields from GAEZ under ‘3 – Agro-climatic Potential Yield’ at <https://gaez.fao.org/pages/data-viewer>, priority areas for biodiversity conservation from <https://zenodo.org/record/5006332#.Y8RrOjMI2w> and water scarcity areas from FAO AQUAMAPS under ‘Distribution of physical water scarcity by major hydrological basin (Global)’ at <https://data.apps.fao.org/aquamaps/>.

Code availability

Custom code used to generate the results reported in this paper is available from the corresponding author upon request. All code is developed in Python and MATLAB.

Received: 1 June 2022; Accepted: 1 February 2023;

Published online: 16 February 2023

References

- Roe, S. et al. Contribution of the land sector to a 1.5°C world. *Nat. Clim. Change* **9**, 817–828 (2019).
- Shukla, P. R. et al. *Climate Change and Land: An IPCC Special Report on climate change, desertification, land degradation, sustainable land management, food security, and greenhouse gas fluxes in terrestrial ecosystems*. (Intergovernmental Panel on Climate Change, 2019).
- Doelman, J. C. et al. Afforestation for climate change mitigation: Potentials, risks and trade-offs. *Glob. Change Biol.* **26**, 1576–1591 (2020).
- Humpenöder, F. et al. Investigating afforestation and bioenergy CCS as climate change mitigation strategies. *Environ. Res. Lett.* **9**, 064029 (2014).
- Popp, A. et al. Land-use futures in the shared socio-economic pathways. *Glob. Environ. Change* **42**, 331–345 (2017).
- Griscom, B. W. et al. Natural climate solutions. *Proc. Natl Acad. Sci.* **114**, 11645–11650 (2017).
- Strassburg, B. B. N. et al. Global priority areas for ecosystem restoration. *Nature* **586**, 724–729 (2020).
- Cook-Patton, S. C. et al. Mapping carbon accumulation potential from global natural forest regrowth. *Nature* **585**, 545–550 (2020).
- Roe, S. et al. Land-based measures to mitigate climate change: Potential and feasibility by country. *Glob. Change Biol.* **27**, 6025–6058 (2021).
- Field, J. L. et al. Robust paths to net greenhouse gas mitigation and negative emissions via advanced biofuels. *Proc. Natl Acad. Sci.* **117**, 21968–21977 (2020).
- Butnar, I., Broad, O., Solano Rodríguez, B. & Dodds, P. E. The role of bioenergy for global deep decarbonization: CO₂ removal or low-carbon energy? *GCB Bioenergy* **12**, 198–212 (2020).
- van Vuuren, D. P. et al. Energy, land-use and greenhouse gas emissions trajectories under a green growth paradigm. *Glob. Environ. Change* **42**, 237–250 (2017).
- Kriegler, E. et al. Fossil-fueled development (SSP5): An energy and resource intensive scenario for the 21st century. *Glob. Environ. Change* **42**, 297–315 (2017).
- Fujimori, S. et al. SSP3: AIM implementation of Shared Socioeconomic pathways. *Glob. Environ. Change* **42**, 268–283 (2017).
- Fricko, O. et al. The marker quantification of the Shared Socioeconomic Pathway 2: A middle-of-the-road scenario for the 21st century. *Glob. Environ. Change* **42**, 251–267 (2017).
- Calvin, K. et al. The SSP4: A world of deepening inequality. *Glob. Environ. Change* **42**, 284–296 (2017).
- Riahi, K. et al. The Shared Socioeconomic Pathways and their energy, land use, and greenhouse gas emissions implications: An overview. *Glob. Environ. Change* **42**, 153–168 (2017).
- Frank, S. et al. Reducing greenhouse gas emissions in agriculture without compromising food security? *Environ. Res. Lett.* **12**, 105004 (2017).
- Kreidenweis, U. et al. Afforestation to mitigate climate change: impacts on food prices under consideration of albedo effects. *Environ. Res. Lett.* **11**, 085001 (2016).
- Zumkehr, A. & Campbell, J. E. Historical U.S. cropland areas and the potential for bioenergy production on abandoned croplands. *Environ. Sci. Technol.* **47**, 3840–3847 (2013).
- Næss, J. S., Cavalett, O. & Cherubini, F. The land–energy–water nexus of global bioenergy potentials from abandoned cropland. *Nat. Sustain.* **4**, 525–536 (2021).
- Milbrandt, A. R., Heimiller, D. M., Perry, A. D. & Field, C. B. Renewable energy potential on marginal lands in the United States. *Renew. Sustain. Energy Rev.* **29**, 473–481 (2014).
- Benayas, J., Martins, A., Nicolau, J. & Schulz, J. Abandonment of agricultural land: An overview of drivers and consequences. *CAB Rev. Perspect. Agric. Vet. Sci. Nutr. Nat. Resour.* **2**, 14 (2007).
- Li, S. & Li, X. Global understanding of farmland abandonment: A review and prospects. *J. Geogr. Sci.* **27**, 1123–1150 (2017).
- Olsson, L. et al. Land degradation. *Clim. Change Land IPCC Spec. Rep. Clim. Change Desertification Land Degrad. Sustain. Land Manag. Food Secur. Greenh. Gas Fluxes Terr. Ecosyst.* (2019).
- Hu, X. et al. Recent global land cover dynamics and implications for soil erosion and carbon losses from deforestation. *Anthropocene* **34**, 100291 (2021).
- Bell, S. M., Barriocanal, C., Terrer, C. & Rosell-Melé, A. Management opportunities for soil carbon sequestration following agricultural land abandonment. *Environ. Sci. Policy* **108**, 104–111 (2020).
- Huang, Y., Li, F. & Xie, H. A scientometrics review on farmland abandonment research. *Land* **9**, 263 (2020).
- Ellison, D. et al. Trees, forests and water: Cool insights for a hot world. *Glob. Environ. Change* **43**, 51–61 (2017).
- Robertson, G. P. et al. Cellulosic biofuel contributions to a sustainable energy future: Choices and outcomes. *Science* **356**, eaal2324 (2017).
- Hanssen, S. V. et al. The climate change mitigation potential of bioenergy with carbon capture and storage. *Nat. Clim. Change* **10**, 1023–1029 (2020).
- Kalt, G. et al. Natural climate solutions versus bioenergy: Can carbon benefits of natural succession compete with bioenergy from short rotation coppice? *GCB Bioenergy* **11**, 1283–1297 (2019).
- Tremblay, S. & Ouimet, R. White spruce plantations on abandoned agricultural land: are they more effective as C sinks than natural succession? *Forests* **4**, 1141–1157 (2013).
- Smith, P. et al. Interlinkages between desertification, land degradation, food security and greenhouse gas fluxes: Synergies, trade-offs and integrated response options. *Clim. Change Land IPCC Spec. Rep. Clim. Change Desertification Land Degrad. Sustain. Land Manag. Food Secur. Greenh. Gas Fluxes Terr. Ecosyst.* **122**, 551–672 (2019).
- Daioglou, V. et al. Greenhouse gas emission curves for advanced biofuel supply chains. *Nat. Clim. Change* **7**, 920–924 (2017).
- Calvin, K. et al. Bioenergy for climate change mitigation: Scale and sustainability. *GCB Bioenergy* **13**, 1346–1371 (2021).
- Voicu, M. F. et al. Carbon dynamics on agricultural land reverting to woody land in Ontario, Canada. *J. Environ. Manage.* **193**, 318–325 (2017).
- Albanito, F. et al. Carbon implications of converting cropland to bioenergy crops or forest for climate mitigation: a global assessment. *GCB Bioenergy* **8**, 81–95 (2016).
- Sochacki, S. J., Harper, R. J. & Smettem, K. R. J. Bio-mitigation of carbon following afforestation of abandoned salinized farmland. *GCB Bioenergy* **4**, 193–201 (2012).
- Mandley, S. J., Daioglou, V., Junginger, H. M., van Vuuren, D. P. & Wicke, B. EU bioenergy development to 2050. *Renew. Sustain. Energy Rev.* **127**, 109858 (2020).
- Sognnaes, I. et al. A multi-model analysis of long-term emissions and warming implications of current mitigation efforts. *Nat. Clim. Change* **11**, 1055–1062 (2021).
- Defourny, P. et al. ESA Land Cover CCI: Product User Guide Version 2.0. (2017).
- Land cover classification gridded maps from 1992 to present derived from satellite observations. *Copernicus Climate Change Service*. <https://cds.climate.copernicus.eu/cdsapp#!/dataset/satellite-land-cover?tab=overview> (2019).
- Leirpoll, M. E. et al. Optimal combination of bioenergy and solar photovoltaic for renewable energy production on abandoned cropland. *Renew. Energy* **168**, 45–56 (2021).
- Chen, M. et al. Global land use for 2015–2100 at 0.05° resolution under diverse socioeconomic and climate scenarios. *Sci. Data* **7**, 320 (2020).
- Friedlingstein, P. et al. Global carbon budget 2022. *Earth Syst. Sci. Data* **14**, 4811–4900 (2022).
- Ritchie, H., Roser, M. & Rosado, P. (2022) - Energy. Published online at OurWorldInData.org. Retrieved from: '<https://ourworldindata.org/energy>' [Online Resource]
- Griscom, B. W. et al. National mitigation potential from natural climate solutions in the tropics. *Philos. Trans. R. Soc. B Biol. Sci.* **375**, 20190126 (2020).
- Olson, D. M. et al. Terrestrial Ecoregions of the World: A New Map Of Life On Earth: a new global map of terrestrial ecoregions provides an innovative tool for conserving biodiversity. *BioScience* **51**, 933–938 (2001).
- Chazdon, R. L. et al. Carbon sequestration potential of second-growth forest regeneration in the Latin American tropics. *Sci. Adv.* **2**, e1501639 (2016).
- Smith, P. et al. Biophysical and economic limits to negative CO₂ emissions. *Nat. Clim. Change* **6**, 42–50 (2016).
- Scott, V., Gilfillan, S., Markusson, N., Chalmers, H. & Haszeldine, R. S. Last chance for carbon capture and storage. *Nat. Clim. Change* **3**, 105–111 (2013).
- Seddou, N. et al. Understanding the value and limits of nature-based solutions to climate change and other global challenges. *Philos. Trans. R. Soc. B Biol. Sci.* **375**, 20190120 (2020).
- Crouzeilles, R. et al. Ecological restoration success is higher for natural regeneration than for active restoration in tropical forests. *Sci. Adv.* <https://doi.org/10.1126/sciadv.1701345> (2017).
- Veldman, J. W. et al. Tyranny of trees in grassy biomes. *Science* **347**, 484–485 (2015).
- Feng, X. et al. Revegetation in China's Loess Plateau is approaching sustainable water resource limits. *Nat. Clim. Change* **6**, 1019–1022 (2016).
- Lautenbach, S. et al. Trade-offs between plant species richness and carbon storage in the context of afforestation – Examples from afforestation scenarios in the Mulde Basin, Germany. *Ecol. Indic.* **73**, 139–155 (2017).
- Rosa, L., Sanchez, D. & Mazzotti, M. Assessment of carbon dioxide removal potential via BECCS in a carbon-neutral Europe. *Energy Environ. Sci.* **14**, 3086–3097 (2021).
- Ai, Z., Hanasaki, N., Heck, V., Hasegawa, T. & Fujimori, S. Global bioenergy with carbon capture and storage potential is largely constrained by sustainable irrigation. *Nat. Sustain.* **4**, 884–891 (2021).
- Rosa, L., Chiarelli, D. D., Rulli, M. C., Dell'Angelo, J. & D'Odorico, P. Global agricultural economic water scarcity. *Sci. Adv.* **6**, eaaz6031 (2020).
- Hong, S. et al. Divergent responses of soil organic carbon to afforestation. *Nat. Sustain.* **3**, 694–700 (2020).

62. Shi, S., Zhang, W., Zhang, P., Yu, Y. & Ding, F. A synthesis of change in deep soil organic carbon stores with afforestation of agricultural soils. *For. Ecol. Manag.* **296**, 53–63 (2013).
63. Don, A., Schumacher, J. & Freibauer, A. Impact of tropical land-use change on soil organic carbon stocks – a meta-analysis. *Glob. Change Biol* **17**, 1658–1670 (2011).
64. Gusti, M., Havlik, P. & Obersteiner, M. 2008. Technical description of the IIASA model cluster, The Eliasch Review; Office of Climate Change. in *Biofuels and LUC in* (2009).
65. Don, A. et al. Land-use change to bioenergy production in Europe: implications for the greenhouse gas balance and soil carbon. *GCB Bioenergy* **4**, 372–391 (2012).
66. Ledo, A. et al. Changes in soil organic carbon under perennial crops. *Glob. Change Biol.* **26**, 4158–4168 (2020).
67. Qin, Z., Dunn, J. B., Kwon, H., Mueller, S. & Wander, M. M. Soil carbon sequestration and land use change associated with biofuel production: empirical evidence. *GCB Bioenergy* **8**, 66–80 (2016).
68. Li, W. et al. Gross and net land cover changes in the main plant functional types derived from the annual ESA CCI land cover maps (1992–2015). *Earth Syst. Sci. Data* **10**, 219–234 (2018).
69. Hua, T., Zhao, W., Liu, Y., Wang, S. & Yang, S. Spatial consistency assessments for global land-cover datasets: a comparison among GLC2000, CCI LC, MCD12, GLOBCOVER and GLCNMO. *Remote Sens* **10**, 1846 (2018).
70. Liu, X. et al. Comparison of country-level cropland areas between ESA-CCI land cover maps and FAOSTAT data. *Int. J. Remote Sens.* **39**, 6631–6645 (2018).
71. Næss, J. S., Jordan, C. M., Muri, H. & Cherubini, F. Energy potentials and water requirements from perennial grasses on abandoned land in the former Soviet Union. *Environ. Res. Lett.* **17**, 045017 (2022).
72. Lesiv, M. et al. Spatial distribution of arable and abandoned land across former Soviet Union countries. *Sci. Data* **5**, 180056 (2018).
73. Baxter, R. E. & Calvert, K. E. Estimating available abandoned cropland in the United States: possibilities for energy crop production. *Ann. Am. Assoc. Geogr.* **107**, 1162–1178 (2017).
74. Alexander, P. et al. Assessing uncertainties in land cover projections. *Glob. Change Biol.* **23**, 767–781 (2017).
75. Kindermann, G. E. et al. Potential stocks and increments of woody biomass in the European Union under different management and climate scenarios. *Carbon Balance Manag* **8**, 2 (2013).
76. Gusti, M. & Kindermann, G. An approach to modeling land use change and forest management on a global scale. in *Proceedings of 1st International Conference on Simulation and Modeling Methodologies, Technologies and Applications* 180–185 (SciTePress - Science and Technology Publications, 2011). <https://doi.org/10.5220/0003607501800185>.
77. Forsell, N. et al. Impact of modelling choices on setting the reference levels for the EU forest carbon sinks: how do different assumptions affect the country-specific forest reference levels? *Carbon Balance Manag* **14**, 10 (2019).
78. Frank, S. et al. Land-based climate change mitigation potentials within the agenda for sustainable development. *Environ. Res. Lett.* **16**, 024006 (2021).
79. Havlik, P. et al. GLOBIOM documentation. *International Institute for Applied Systems Analysis (IIASA)*. (Laxenburg, Austria, 2018).
80. Avitabile, V. & Camia, A. An assessment of forest biomass maps in Europe using harmonized national statistics and inventory plots. *For. Ecol. Manag.* **409**, 489–498 (2018).
81. Böttcher, H., Verkerk, P. J., Gusti, M., Havlík, P. & Grassi, G. Projection of the future EU forest CO₂ sink as affected by recent bioenergy policies using two advanced forest management models. *GCB Bioenergy* **4**, 773–783 (2012).
82. Böttcher, H., Verkerk, H., Gusti, M., Havlik, P. & Schneider, U. A. *Analysis of potential and costs of LULUCF use by EU Member States*. (2011).
83. Li, W. et al. Mapping the yields of lignocellulosic bioenergy crops from observations at the global scale. *Earth Syst. Sci. Data* **12**, 789–804 (2020).
84. Crawford, C. L. et al. Rural land abandonment is too ephemeral to provide major benefits for biodiversity and climate. *Sci. Adv.* **8**, eabm8999 (2022).
85. Yin, H. et al. Monitoring cropland abandonment with Landsat time series. *Remote Sens. Environ.* **246**, 111873 (2020).
86. Santoro, M. et al. ESA Land Cover CCI: Product User Guide Version 1.1. (2017).
87. Defourny, P., Lamarche, C. & Marissiaux, Q. Product user guide and specification. *ICDR Land Cover 2016–2020*, 37 (2021).
88. Defourny, P., Lamarche, C. & Marissiaux, Q. Product quality assessment report. *ICDR Land Cover 2016–2020*. (2020).
89. Popp, A. et al. Land-use protection for climate change mitigation. *Nat. Clim. Change* **4**, 1095–1098 (2014).
90. Lotze-Campen, H. et al. Scenarios of global bioenergy production: The trade-offs between agricultural expansion, intensification and trade. *Ecol. Model.* **221**, 2188–2196 (2010).
91. Bayer, A. D. et al. Diverging land-use projections cause large variability in their impacts on ecosystems and related indicators for ecosystem services. *Earth Syst. Dyn.* **12**, 327–351 (2021).
92. Hurtt, G. C. et al. Harmonization of global land use change and management for the period 850–2100 (LUH2) for CMIP6. *Geosci. Model Dev.* **13**, 5425–5464 (2020).
93. Brown, C., Holman, I. & Rounsevell, M. How modelling paradigms affect simulated future land use change. *Earth Syst. Dyn.* **12**, 211–231 (2021).
94. Meyfroidt, P., Schierhorn, F., Prishchepov, A. V., Müller, D. & Kuemmerle, T. Drivers, constraints and trade-offs associated with recultivating abandoned cropland in Russia, Ukraine and Kazakhstan. *Glob. Environ. Change* **37**, 1–15 (2016).
95. Schierhorn, F. et al. Post-Soviet cropland abandonment and carbon sequestration in European Russia, Ukraine, and Belarus. *Glob. Biogeochem. Cycles* **27**, 1175–1185 (2013).
96. Alcantara, C. et al. Mapping the extent of abandoned farmland in Central and Eastern Europe using MODIS time series satellite data. *Environ. Res. Lett.* **8**, 035035 (2013).
97. Hu, X., Huang, B., Veronesi, F., Cavalett, O. & Cherubini, F. Overview of recent land-cover changes in biodiversity hotspots. *Front. Ecol. Environ.* **19**, 91–97 (2021).
98. Barthlott, W., Mutke, J., Rafiqpoor, M. D., Kier, G. & Kreft, H. Global centers of vascular plant diversity. *Nova Acta Leopoldina* **92**, 61–83 (2005).
99. Stenzel, F. et al. Irrigation of biomass plantations may globally increase water stress more than climate change. *Nat. Commun.* **12**, 1512 (2021).
100. FAO. AQUASTAT - FAO's Global Information System on Water and Agriculture. <https://data.apps.fao.org/aquamaps/> (2010).
101. Næss, J. S. et al. Climate change mitigation potentials of biofuels produced from perennial crops and natural regrowth on abandoned and degraded cropland in Nordic countries. *J. Environ. Manage.* **325**, 116474 (2023).
102. Kindermann, G., McCallum, I., Fritz, S. & Obersteiner, M. A global forest growing stock, biomass and carbon map based on FAO statistics. *Silva Fenn* **42**, 387–396 (2008).
103. Gusti, M. I. An algorithm for simulation of forest management decisions in the global forest model. *Штучний інтелект* (2010).
104. Gusti, M., Di Fulvio, F., Biber, P., Korosuo, A. & Forsell, N. The effect of alternative forest management models on the forest harvest and emissions as compared to the forest reference level. *Forests* **11**, 794 (2020).
105. Schelhaas, M.-J. et al. Forest resource projection tools at the European level. in *Forest Inventory-based Projection Systems for Wood and Biomass Availability* (eds. Barreiro, S., Schelhaas, M.-J., McRoberts, R. E. & Kändler, G.) 49–68 (Springer International Publishing, 2017). https://doi.org/10.1007/978-3-319-56201-8_4.
106. Döschner, R. et al. The EC-Earth3 earth system model for the coupled model intercomparison project 6. *Geosci. Model Dev.* **15**, 2973–3020 (2022).
107. Billard, A. et al. Improving aboveground biomass estimates by taking into account density variations between tree components. *Ann. For. Sci.* **77**, 103 (2020).
108. Segura, M. & Kanninen, M. Allometric models for tree volume and total aboveground biomass in a tropical humid forest in Costa Rica. *Biotropica* **37**, 2–8 (2005).
109. Peichl, M. & Arain, M. A. Allometry and partitioning of above- and belowground tree biomass in an age-sequence of white pine forests. *For. Ecol. Manag.* **253**, 68–80 (2007).
110. Cavalett, O. & Cherubini, F. Contribution of jet fuel from forest residues to future Sustainable Development Goals. *Nat. Sustain.* **1**, 799–807 (2018).
111. Lewandowski, I., Clifton-Brown, J. C., Scurlock, J. M. O. & Huisman, W. Miscanthus: European experience with a novel energy crop. *Biomass Bioenergy* **19**, 209–227 (2000).
112. Heinsoo, K., Hein, K., Melts, I., Holm, B. & Ivask, M. Reed canary grass yield and fuel quality in Estonian farmers' fields. *Biomass Bioenergy* **35**, 617–625 (2011).
113. Lewandowski, I. & Schmidt, U. Nitrogen, energy and land use efficiencies of miscanthus, reed canary grass and triticale as determined by the boundary line approach. *Agric. Ecosyst. Environ.* **112**, 335–346 (2006).
114. Parrish, D. J. & Fike, J. H. The biology and agronomy of switchgrass for biofuels. *Crit. Rev. Plant Sci.* **24**, 423–459 (2005).
115. Fischer, G. et al. Global Agro-Ecological Zones (GAEZ v4) Model Documentation. *FAO & IIASA*, 303 (2021).
116. TNO Biobased and Circular Technologies. Phyllis2 - Database for the physico-chemical composition of (treated) lignocellulosic biomass, micro- and macroalgae, various feedstocks for biogas production and biochar. <https://phyllis.nl/>.
117. Transport Biofuels. *IEA*. <https://www.iea.org/reports/transport-biofuels> (2021).
118. Jordan, C.-M. et al. Energy potentials, negative emissions, and spatially explicit environmental impacts of perennial grasses on abandoned cropland in Europe. *Environ. Impact Assess. Rev.* **98**, 106942 (2023).
119. Kiesel, A., Wagner, M. & Lewandowski, I. Environmental performance of miscanthus, switchgrass and maize: can C4 perennials increase the sustainability of biogas production? *Sustainability* **9**, 5 (2017).

120. Murphy, F., Devlin, G. & McDonnell, K. Miscanthus production and processing in Ireland: An analysis of energy requirements and environmental impacts. *Renew. Sustain. Energy Rev.* **23**, 412–420 (2013).
121. Morales, M., Arvesen, A. & Cherubini, F. Integrated process simulation for bioethanol production: Effects of varying lignocellulosic feedstocks on technical performance. *Bioresour. Technol.* **328**, 124833 (2021).
122. Wernet, G. et al. The ecoinvent database version 3 (part I): overview and methodology. *Int. J. Life Cycle Assess.* **21**, 1218–1230 (2016).
123. Lask, J., Wagner, M., Trindade, L. M. & Lewandowski, I. Life cycle assessment of ethanol production from miscanthus: A comparison of production pathways at two European sites. *GCB Bioenergy* **11**, 269–288 (2019).
124. Swanson, R. M., Platon, A., Satrio, J. A. & Brown, R. C. Techno-economic analysis of biomass-to-liquids production based on gasification. *Fuel* **89**, S11–S19 (2010).
125. Oreggioni, G. D. et al. Environmental assessment of biomass gasification combined heat and power plants with absorptive and adsorptive carbon capture units in Norway. *Int. J. Greenh. Gas Control* **57**, 162–172 (2017).
126. McAllister, S., Chen, J.-Y. & Fernandez-Pello, A. C. *Fundamentals of Combustion Processes*. (Springer New York, 2011). <https://doi.org/10.1007/978-1-4419-7943-8>.
127. Edwards, R. et al. *Definition of input data to assess GHG default emissions from biofuels in EU legislation*. (2016). <https://doi.org/10.2790/38877>.

Acknowledgements

We acknowledge the support of the Norwegian Research Council through the projects BioPath (294534), MITISTRESS (286773), Bio4Fuels (257622), and BEST (288047). The simulations were performed on resources provided by the Industrial Ecology Digital Laboratory at NTNU. We thank Bo Huang for his contribution with data acquisition and pre-processing input climate data, Martin Dorber for the gridded version of the terrestrial ecoregions, and Kajwan Rasul for his advice during code development.

Author contributions

M.H.G., J.S.N., and F.C. designed the study. M.H.G. produced and analyzed the results and led the writing of the paper. F.C. contributed to writing the paper and the supplementary information. X.H. and J.S.N. contributed with data analysis and validation. M.D.B.W. and O.C. contributed with inventory data for bioenergy production, M.M. with projections of future land cover data, and G.K. with G4M afforestation data. All authors contributed to interpret the results and edit the paper.

Funding

Open access funding provided by Norwegian University of Science and Technology.

Competing interests

The authors declare no competing interests.

Additional information

Supplementary information The online version contains supplementary material available at <https://doi.org/10.1038/s43247-023-00696-7>.

Correspondence and requests for materials should be addressed to Maren H. Gvein or Francesco Cherubini.

Peer review information *Communications Earth & Environment* thanks Wei Li and the other, anonymous, reviewer(s) for their contribution to the peer review of this work. Primary Handling Editors: Jinfeng Chang and Clare Davis. Peer reviewer reports are available.

Reprints and permission information is available at <http://www.nature.com/reprints>

Publisher's note Springer Nature remains neutral with regard to jurisdictional claims in published maps and institutional affiliations.



Open Access This article is licensed under a Creative Commons Attribution 4.0 International License, which permits use, sharing, adaptation, distribution and reproduction in any medium or format, as long as you give appropriate credit to the original author(s) and the source, provide a link to the Creative Commons license, and indicate if changes were made. The images or other third party material in this article are included in the article's Creative Commons license, unless indicated otherwise in a credit line to the material. If material is not included in the article's Creative Commons license and your intended use is not permitted by statutory regulation or exceeds the permitted use, you will need to obtain permission directly from the copyright holder. To view a copy of this license, visit <http://creativecommons.org/licenses/by/4.0/>.

© The Author(s) 2023